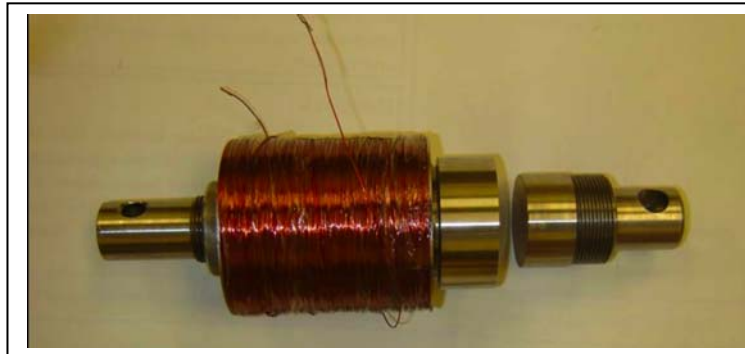# PROJECT PROFILE

Study on the Conformational Behaviour of Magnetorheological Fluid in Squeeze Mode

Research Area: Material's Behaviour

Saiful Amri bin Mazlan
Aminudin bin Abu
Mohd Yusof bin Md Daud
Hairi bin Zamzuri

Materials & Manufacturing Research Alliance

Universiti Teknologi Malaysia

amri@ic.utm.my

STUDY ON THE CONFORMATIONAL BEHAVIOUR OF MAGNETORHEOLOGICAL FLUID IN SQUEEZE MODE

(PEMBUKTIAN KELAKUAN BENDALIR MAGNETORHEOLOGICAL DI BAWAH PENGARUH DAYA TEKANAN)

SAIFUL AMRI BIN MAZLAN
AMINUDIN BIN ABU
MOHD YUSOF BIN MD DAUD
HAIRI BIN ZAMZURI

RESEARCH VOTE NO:

77923

RAZAK SCHOOL OF ENGINEERING
AND ADVANCED TECHNOLOGY
UNIVERSITI TEKNOLOGI MALAYSIA

2011

DEDICATION

ABSTRACT

STUDY ON THE CONFORMATIONAL BEHAVIOUR OF MAGNETORHEOLOGICAL FLUID IN SQUEEZE MODE

This study intends to address the lack of awareness regarding magnetorheological (MR) fluids behaviour in squeeze mode. The aim of this study is to provide a thorough investigation of the microstructure of MR fluid under compression. The explanation to the numerous commercial applications of MR fluids lies in their reversible rheological transition in which is thoroughly linked to the drastic transformation in suspension microstructures. The success of MR fluid is apparent in many disciplines, ranging from the automotive and civil engineering communities to the biomedical engineering community. MR fluids operated in squeeze mode have unique features as a result of its ability to produce much higher compressive and tensile stresses. This research has identified the compression behaviour of MR fluids under squeeze mode. The compression behaviour of the epoxy-based MR fluid was examined throughout compression tests of 25%, 50% and 75%. The compressive stress recorded under compression of 75% was significantly higher than under compression of 50%. Meanwhile, under compression of 25%, the compressive stress showed only a slight increased in comparison. In addition, the compressive stresses plotted by 20% volume fraction of carbonyl iron particle (CIP) were always higher than 10% volume fraction of CIP. Therefore, the higher the volume fraction of CIP and the compressive strain, the higher compressive stress of MR fluids would be achieved. During compression, the volume fractions of CIP of the MR fluids have shown an increase as a result of relative decrease in the volume of samples composition. In the microstructure analysis, the particles distributions and column sizes of the specimens were found to increase in conjunction with the compression and recorded a significant value under compression of 75%. This microstructure study proves that during the compression, most of the CIP were hold in the fluids while the epoxy was expelled out of the compression area.

(Keywords: Magnetorheological fluids, squeeze mode, compression, microstructure)

Key researchers:

Ir. Dr. Saiful Amri Mazlan (Head)
Dr. Aminudin Abu
Dr. Mohd Yusof Md Daud
Dr. Hairi Zamzuri

E-mail: amri@ic.utm.my
Tel. No.: 03-26154607
Vote No.: 77923

ABSTRAK

PEMBUKTIAN KELAKUAN BENDALIR MAGNETORHEOLOGICAL DI BAWAH PENGARUH DAYA TEKANAN

Kajian ini dijalankan untuk meningkatkan pengetahuan berkenaan sifat bendalir magnetorheological (MR) di bawah pengaruh daya tekanan. Objektif kajian ini adalah bertujuan untuk memeriksa mikrostuktur bendalir secara terperinci apabila tekanan dikenakan. Banyak kegunaan bendalir MR bergantung kepada sifat boleh-ubah di mana ianya mengalami perubahan yang terlalu pantas di dalam mikrostuktur bahan apabila dimampatkan. Bendalir MR telah berjaya di gunakan di dalam pelbagai bidang merintangi bidang automotif dan kejuruteraan awam, sehingga ke cabang kejuruteraan bio-perubatan. Bendalir MR yang berfungsi secara dinamik mempunyai daya mampatan serta daya terikan yang amat besar. Secara keseluruhan, kajian telah berjaya mendapatkan sifat bendalir MR di bawah tekanan dinamik. Sifat bendalir MR yang berlandaskan epoxy telah dikaji melalui mampatan pada peringkat 25%, 50% dan 75% daripada keseluruhan proses mampatan. Ujikaji menunjukkan bahawa daya mampatan pada 75% adalah lebih tinggi dari daya mampatan pada 50%. Pada ujikaji yang lain, daya mampatan pada 25% hanya menunjukkan peningkatan yang sedikit sahaja jika dibandingkan dengan daya-daya mampatan pada peringkat yang lain. Sebagai tambahan, daya mampatan bagi 20% carbonyl iron particle (CIP) adalah lebih tinggi dari 10% CIP. Oleh itu, semakin tinggi pecahan CIP dan terikan yang akan diuji, semakin tinggi daya mampatan yang bakal diperolehi. Semasa proses mampatan, pecahan isipadu CIP di dalam bendalir MR menunjukkan kenaikan selaras dengan pengurangan isipadu sampel bahan ujikaji. Taburan partikel dan saiz kolum sampel ujikaji secara mikrostruktur adalah lebih banyak dan besar, dan keadaan ini bersesuaian dengan mampatan yang diperolehi pada 75%. Hasil keputusan yang diperolehi daripada kajian mikrostuktur telah membuktikan bahawa semasa proses mampatan, kebanyakkan CIP dikekalkan bersama bendalir MR manakala epoxy telah keluar dari kawasan mampatan.

TABLE OF CONTENTS

CHAPTER 7: HUMAN CAPITAL DEVELOPMENT   **53**

CHAPTER 8: AWARDS / ACHIEVEMENT   **53**

LIST OF TABLES

LIST OF FIGURES

FIGURES OF CHAPTER 4

NOMENCLATURES

η	:	Viscosity
B	:	Magnetic flux density
H	:	Magnetic field intensity
M	:	Magnetization of the material
I	:	Current
h	:	Height of the gap
r	:	Radius
V	:	Volume
F	:	Force
P	:	Pressure
τ	:	Shear stress
τ_y	:	Yield stress
γ	:	Shear strain
$\dot{\gamma}$	:	Shear strain rate
u	:	Velocity of the particles
G	:	Complex material modulus
ρ	:	Density of the fluid
w	:	Weight percentage

LIST OF APPENDICES

These appendices are divided into two sections:

A. The Stress-Strain Relationships of epoxy based MR fluids

B. The SEM images of epoxy based MR Fluids in 'off' state, 'on' state and under compression of 25%, 50% and 75%

FIGURE OF APPENDIX A

FIGURES OF APPENDIX B

CHAPTER 1

INTRODUCTION

1.1 Introduction

About sixty years ago, a new class of materials, thereafter called smart materials, were discovered and developed. These are field-responsive fluids that demonstrate a rapid, reversible and tuneable transformation upon the induction of an external field, from a liquid-like free-flowing state to a solid-like state, which shows a high resistance to flow. The unique transforms emerging in the structure and rheological properties of these fluids upon the application of an electric or a magnetic field give them the name of electrorheological (ER) or magnetorheological fluids, respectively.

Magnetorheological suspensions are formed by micron-sized ferromagnetic particles dispersed in a non-magnetic carrier fluid. In the absence of an external field, and at low volume fractions, these suspensions behave as Newtonian-like fluids. However, when a magnetic field is applied, a magnetic dipole moment is induced in the particles. The magnetic interaction between the resulting induced dipoles causes the particle to aggregate forming chains aligned in the field direction. These structures restrict the motion of the fluid, thereby increasing the viscosity of the suspension. The apparent deformation resistance and the rheological properties of these fluids can be altered significantly and continuously within milliseconds.

The MR fluids offers three modes of operation depending on the type of deformation engaged, these being valve (or flow) mode, shear mode and squeeze mode. These modes involve, respectively, MR fluid flowing as a result of pressure different between two stationary plates; MR fluid between two plates moving relative to one another; and MR fluid is squeezed out of a narrowing gap between two plates. In all modes, the magnetic field is applied perpendicular to the planes of the plates in order to control the fluid in the direction parallel to the plates.

1.2 Motivation of Study

Magnetorheological (MR) fluids offer solutions to various engineering applications. The success of MR fluid is apparent in many disciplines, ranging from the automotive and civil engineering communities to the biomedical engineering community. Practical interest in these fluids derives from their excellent ability of precise controllability and to provide for rapid-response interfaces between electronic controls and mechanical systems, which make them especially useful in control devices [1]. Moreover, energetic reasons favour their use within control devices, because these suspensions may be used to control hundreds of Watts of mechanical power using only a few Watts of electric power. Furthermore, the control precision of MR fluids products in comparison is 20 to 50 times greater than the equivalent ER fluids products [1]. The performance of today's MR fluids and devices is the outcome of a great number of research works, which identify the properties and behaviours of MR fluids.

Among the three working modes, the investigation of the MR fluids behaviour in squeeze mode is so far hardly discussed in literature. Correspondingly, the commercial applications of MR fluids in the squeeze mode are limited to small amplitude vibration damping, due to the lack of understanding of the material behaviour [2,3]. On the other hand, MR fluids operated in squeeze mode have unique features due to its ability to produce much higher compressive and tensile stresses and also its suitability for applications of controlling small, millimetre-order movements but involving large forces [3]. For this reason, the study of MR fluids in squeeze mode has received considerable attention in recent years.

The explanation to the numerous commercial applications of MR fluids lies in their reversible rheological transition in which is thoroughly linked to the drastic transformation in suspension microstructure. The microstructures change that takes place upon the application of a magnetic field is just a transformation from a medium formed by isotropic structures to a medium in which the particles form chains parallel to the applied field (anisotropic structures). Therefore, detailed information of the suspension's microstructure upon the application of magnetic fields and under compression in squeeze mode in particular is essential in order to understand and control its rheological response.

1.3   Objectives

This study intends to address the lack of awareness regarding MR fluids behaviour in squeeze mode. The aim here is to provide a thorough investigation of the microstructure of MR fluid under compression. The primary objectives of this research can be summarised as follows:

(a)   To produce solidified epoxy based MR fluids through compression tests.

(b)   To study the stress-strain relationships of MR fluids under compression.

(c)   To investigate the compression behaviour of MR fluids in squeeze mode through microstructure study.

1.4   Layout of Report

This report is organised in six chapters. Chapter 1 provides a brief introduction on MR fluids and their fundamental properties. This chapter also provides the motivation of study and outlines the objectives of this project. The next chapter, Chapter 2, provides background on MR fluids and their applications. A general discussion of the most fundamental behaviour of MR fluids is presented. Chapter 2 also discusses the commercial applications of MR fluids in several industries. In Chapter 3, the experimental approach is introduced, started with the materials preparation followed by compression tests and finally SEM analysis. Results for the viscosity tests, compression tests and SEM analysis are presented in Chapter 4. This chapter discusses, in detail, the compression behaviour of MR fluids in squeeze mode from the microstructure point of view. Finally, Chapter 5 provides conclusion of the study and highlights the significant results.

CHAPTER 2

LITERATURE REVIEW

2.1   Introduction

Advances in the application of MR fluids are in line with the development of new, more sophisticated MR materials with better properties and stability. In recent years, the study of MR fluids behaviour in squeeze mode has received particular interest due to the fact that the literature and fundamental knowledge in this working mode are still limited [1,3,4]. Moreover, MR fluids in squeeze mode has highly non-linear behaviour, which is still not fully understood and therefore expected to give rise to new industrial applications. The well-known advantage of MR fluids in squeeze mode is their capability to produce much higher compressive and tensile stresses amongst other modes [1,3]. Therefore, MR fluids in squeeze mode are suitable for many applications requiring a large range of controllable force but only involving small strokes.

Compression is one of the mechanisms in the squeeze mode. Similar to ER fluids, it was reported that the performance of compressive stress of MR fluids was the greatest among other stresses [5]. For that reason, it is essential to investigate the compression behaviour of MR fluids in squeeze mode in order to find out the achievable stress. For that purpose, a detailed knowledge of the relationships of compressive stress-strain and the suspension's microstructure in the compression mode is considered necessary. This can be done respectively by conducting compressions tests and using scanning electron microscopy (SEM) to examine the particle size, particle size distribution, column size and surface morphology of the particles. Further study of the behaviour of MR fluids during the compression process concerning the relative movement between the iron particles and the carrier liquid will be advantage.

2.2   Field-Responsive Fluids

Smart materials have some properties, which can be significantly altered or tuned in a controlled fashion using some external fields. These include materials that demonstrate ferroelectricity, pyroelectricity, piezoelectricity, a shape memory effect, electrostriction, magnetostriction, electrochromism, photomagnetism and photochromism [6]. There is also a class of smart materials identified as 'field-responsive fluids'. These fluids are consisting of ferrofluids, ER fluids, MR fluids and certain types of polymeric gels. These materials are dissimilar from the traditional smart materials, in that they are soft materials (typically dispersions or gels) rather than solids [3,6].

Basically, an ordinary property of field-responsive fluids these is that, they are all distributions of particles in a carrier liquid and some portion of their rheology is controlled by an external electric or magnetic field. The rheological transformation is rapid, controllable and completely reversible. In the case of ferrofluids, generally they do not build particle chains but experience a body force on the entire fluids, which cause the fluids to be attracted to regions of high magnetic field strength [6]. Meanwhile, MR fluids and ER fluids require the use of solid

particles that are magnetisable and responsive to an electric field, respectively. Generally, MR and ER fluids have complementary advantages and disadvantages; thereby they have different applications and market demand. The significant advantage of MR fluids is their ability to produce higher stresses that they can withstand, while the main advantage of ER fluids is that they can be developed and operated in a smaller system [3].

It is interesting to note that, with the exclusion of the last ten years or so, after their early breakthrough and a flurry of activity that followed, the study into MR fluids essentially came to a stand-still while the research in ER fluids continued [2]. In contrast, although ferrofluids were invented after ER and MR fluids, they found their way into the marketplace relatively fast. The relatively higher interest and enthusiasm related with ER fluids as well as problems associated with the quality of some of the early MR fluid compositions may have been contributing factors to the situation. Particularly, the inability of the ferromagnetic iron particles to remain in suspension was concerned [6].

### a)	*Ferrofluids*

Ferrofluids are well known as magnetic liquids or liquid magnets that are colloidal suspensions of ultra-fine (typically 5-10 nm), single domain magnetic particles such as iron oxides (γFe_2O_3, Fe_3O_4), Mn-Zn ferrites, Fe and Co in either aqueous or non-aqueous liquids [6,7]. Since the particle size of the magnetic phase is very small, under normal field strengths, thermal energy gives increase to Brownian forces that can conquer the alignment of the dipoles. Accordingly, ferrofluids are based on superparamagnetic materials, while MR fluids are based on ferromagnetic or ferromagnetic particles [7]. Instead, ferrofluids experience a body force on the material as a whole that is proportional to the magnetic field gradient. As a result, in a superparamagnetic material, the magnetic dipole moment changes its direction very quickly and hence the entire particle does not exhibit a net time averaged dipole moment. In another word, ferrofluids exhibit no yield stress under magnetic fields but field dependent viscosity [6,7].

In comparison, the stability of ferrofluids is much greater than MR fluids, which are based on non-colloidal magnetic particles [8]. However, ferrofluids have smaller particles than MR fluids particles and have different responses under the same amplitude of applied magnetic field. Ferrofluids and devices based on ferrofluids are commercially successful, and are mainly used as high pressure seals and rotary seals, magnetic bearings, motor dampers, cooling medium, electronic devices, heat dissipation and biomedical devices [6,8]. Figure 2.1 shows a ferrofluidic inertia damper manufactured by Ferrotec (USA).
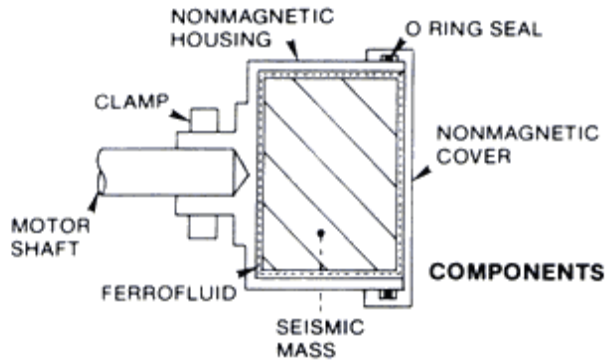
Figure 2.1. Ferrotec's ferrofluidic inertia damper [9].

b)   *Electrorheological (ER) Fluids*

ER fluids are identified as suspensions of electrically polarizable particles dispersed in electrically insulating oil. Typically, the ER fluid is composed of 0.5 to 100 μm particles of cornstarch, silica, barium titanate or semiconductors [5,7]. In order to enhance the ER effect, for particles such as silica, polyelectrolytes require to be supplemented to cause the adsorption of water onto the particulate material, thus increasing the electrostatic strength of attraction between the particles. The water also produces a conductive layer on the surface of the particles in which the ions in the water can drift in response to an electric field [5,7]. These materials are called extrinsically polarizable materials wherein the ER effect results from interfacial polarization. The ER effect decreases as the amount of water absorbed decreases. For that reason, at temperatures of about 50^0C, the ER activity decreases significantly and as a result the temperature instability restrict the potential application of the ER fluids [7].

Upon the application of electric field, the ER fluids particles became polarized and the local electric field was distorted. An ordinary accepted mechanism to describe the development of an apparent yield stress was that the applied electric field results in inducement of dipoles in the dielectric particles and the particles with induced dipoles experience alignment to minimise the dipole-dipole interaction energy [5,7]. The polarizability of the particles was enhanced by the movement of the mobile charges to regions with greatest field concentration. This gave increased to larger dipole moments that attracted one another and caused the particles to build chain network in the direction of the field. Consequently, these particle chains restricted the movement of the suspension. ER fluid could be characterized by the Bingham Plastic Model, in which the alteration in viscosity from particle chain interactions under shear corresponded to the yield stress. Weiss and co-workers revealed a yield stress value of 3.5 kPa for 4kV/mm of electric field for one of the Lord Corporation's ER fluids (VersaFlo ER 200) [7].

Since the invention of ER fluids about 60 years ago, a great deal of research and development works has gone into the development of their application and devices [5,7]. Unfortunately, these efforts have not resulted in a great number of commercially successful devices. The explanation for the lack of any significant commercial success could be the lower yield stresses, the temperature dependence of yield stress, sensitivity of ER fluids to impurities

5

(which can change polarisation mechanisms), and the required for relatively expensive high voltage supplies which were not always very robust [6]. ER fluids were mostly developed for valves, mount, clutch, brake, and damper, although not much advancement has been made in their commercialization. Figure 2.2 shows the ER fluids based damper manufactured by Bansbach (Germany).

Figure 2.2. Bansbach's easyERF damper [10].

c)   *Magnetorheological (MR) Fluids*

MR fluids are suspensions that contain mesoscale (l-10 μm) ferromagnetic or ferromagnetic particulates dispersed in an organic or aqueous carrier liquid [2,11]. A variety of ceramic metals and alloys can be used to prepare MR fluids as long as the particles are magnetically multi-domain and show low levels of magnetic coercivity. High purity iron (Fe) powder derived from decomposition of iron penta-carbonyl ($Fe(CO)_5$) is the most regular magnetic material used to prepare the MR fluids [6,11]. The essential features of the magnetically active dispersed phase are particle size, particle size distribution, shape, density, saturation magnetization and coercive field. Besides that, other vital factors that affect the rheological properties such as stability and redispersibility of the MR fluid are carrier fluids, surfactants and additives [7].

In the "off" state, MR fluids appeared comparable to liquid paints and exhibit equivalent levels of apparent viscosity when their consistency was considered. When a magnetic field was applied, the originally magnetic particles become magnetised and become almost single domain and behave like tiny magnets, consequently their apparent viscosity altered rapidly within a few milliseconds. In order to minimise the magnetic interactions between these particles, the magnetic particles line-up along the direction of the magnetic field [6,11]. This dipolar interaction was leading to the chain like formation of the particles in the direction of the magnetic field, as shown in figure 2.3. The strength of the apparent yield stress increased as the applied magnetic field increased. The alteration in the viscosity was completely reversible when the magnetic field was removed.
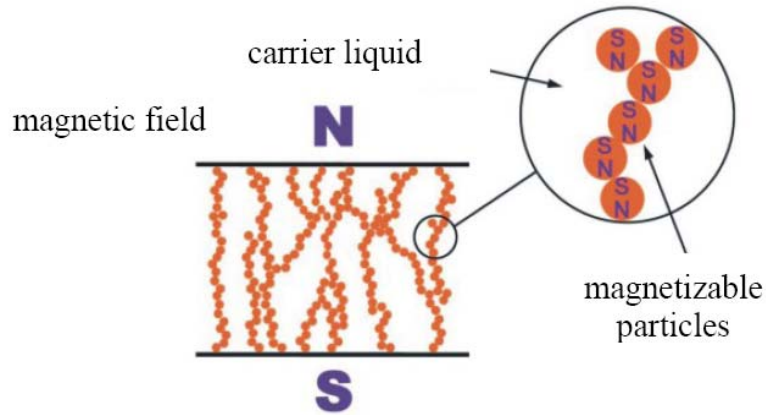
Figure 2.3. Formation of chain-like structures in MR fluids [11].

MR fluids were able to develop an apparent yield stress up to about 50-100 kPa, depending on their composition and the flux density generated by the applied magnetic field [11,12]. In order to increase in the maximum apparent yield stress, higher saturation magnetisation materials could be optimised; unfortunately the availability and cost of such materials might be a limiting factor. MR fluids represent one of the fastest electro-mechanical interfaces, since the development of yield stress in MR fluids could be occurred within a few milliseconds, and provided that the electrical circuit generating the magnetic field was optimised [6]. MR technology has moved out of the laboratory and into viable commercial applications for a miscellaneous of products such as in the automotive, aerospace, robotic, acoustic, and biomedical engineering fields [13].

d) *Comparison of Field-Responsive Fluids*

More recently, MR fluids have gained considerably more attention than their electric analogue ER fluids. One of the significant advantages of MR fluids is the higher yield stress magnitude than ER fluids, due to its higher magnetostatic energy density. Secondly, the MR fluids require smaller amount of active fluids as compared to ER fluids to perform mechanical performance [3,7]. Correspondingly, MR fluids need only small voltages and high currents, while ER fluids demand high voltages and low currents for the same required magnitude of power. Low voltage power supplies for MR fluids and relative temperature stability put them more attractive materials than ER fluids. On the contrary, ER fluids have an advantage where they show higher response characteristics rather than MR fluids.

On the other hand, even though ferrofluids show an increase in the viscosity, they do not exhibit yield stress. The viscosity under an applied magnetic field increases almost double from the initial magnitude when the fluids in 'off' state. Since ferrofluids are synthesized by colloidal magnetic particles, these fluids have more stability than MR fluids, which are based on non-colloidal magnetic particles [6,7]. The comparison of ferrofluids, ER fluids, and MR fluids is summarized in table 1.

Table 1. Comparison of some properties of Ferrofluids, ER fluids and MR fluids [7].

No.	Items	Ferrofluids	ER Fluids	MR Fluids
1	Particulate material	Ceramics, ferrites, iron, cobalt, etc.	Zeolites, polymers, SiO_2, $BaTiO_3$	Iron, ferrites, etc
2	Particle size	2-10 nm	0.1-10μm	0.1-10μm
3	Carrier fluids	Oils, water	Oils	Non-polar oils, polar liquids, water and other
4	Density (g/cc)	1-2	1-2	3-5
5	Off viscosity (mPa-s)	2-500	50-1000	100-1000
6	Required field	~1 kOe	3kV/mm	~ 3 kOe
7	Field induced changes		τ_y (E) ~ 10 kPa	τ_y (B) ~100kPa
8	Device excitation	Permanent magnet	High voltage	Electromagnets or permanent magnet

2.3   Composition of MR Fluids

MR fluids are non-colloidal suspensions of micron-sized, magnetically polarizable particles, typically within 0.1-10 µm in diameter. These particles are suspended in some form of carrier liquid, usually selected based upon their rheological properties and temperature stability. In order to enhance the performance and durability of MR fluids, the additives may be used. Each component of the fluid (the iron particles, the carrier fluid, and additives) greatly influences the 'off' state behaviour of the fluid and will be discussed briefly in the following text.

a)   *Iron particles*

Normally, the major compositions in many of the MR fluids consist of 20-40% by volume of carbonyl iron powder. Iron powder is the most popular material used as a result of its high saturation magnetization and magnetic softness [11,15]. Moreover, carbonyl iron is chemically pure and the particles are meso-scale and spherical in nature. These soft iron particles are produced from the thermal decomposition of iron penta-carbonyl ($Fe(CO)_5$) and are remarkably spherical in shape [6, 11], as shown in figure 2.4.
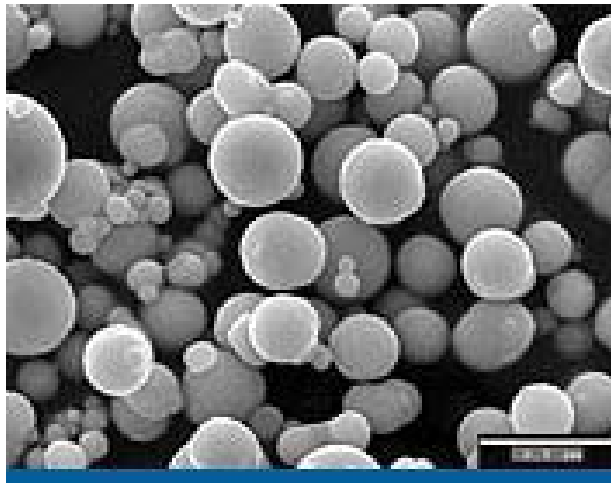
Figure 2.4. SEM image of carbonyl iron powder [16].

The meso-scale particles are useful and practical since they have lots of magnetic domains. The high level of chemical purity provides less domain pinning defects, while the spherical shape assists to minimise the magnetic shape anisotropy [6,11]. High purity iron powders are more suitable due the MR fluids based devises preferred to have particles that are non-abrasive. Other magnetic materials, which are appropriate to be used to prepare MR fluids, are ferromagnetic and ferromagnetic materials such as iron-cobalt alloys, manganese zinc ferrite and nickel zinc ferrite [11].

b)   *Carrier liquids*

The carrier liquid acts an essential role to provide a liquid in which the magnetically active phase particulates are suspended. Normally, relative volume fractions of the liquid phase range approximate from 50 to 90 percent [6]. Petroleum based oils, mineral oils, silicone oils, synthetic or semi-synthetic oils, lubricating oils and combinations of these and many other polar organic liquids and water have all been reported are suitable to be used as carrier liquids [11]. High consideration must be put to several features such as the boiling temperature, vapour pressure at elevated temperatures and freezing point before a carrier liquid is selected. In addition, the carrier liquid should also be basically non-reactive towards the magnetic particles and the components or materials used in the device as well.

Another important factor that must be considered is to select the carrier fluids that do not show significant variation in the 'off-state' viscosity at a given temperature. However, the variation of viscosity as a function of temperature may also be considered. Finally, another option to be considered is in a condition where there is no carrier liquid required. The so-called 'dry' MR fluids play as magnetic particle breaks, for instance dry powders of ferromagnetic materials such as magnetic stainless steel are used in various commercial devices for many years [6].

9

c) *Additives in MR fluids*

In order to improve the durability of MR fluids and enhance their devices' performance, additives can be supplemented into the smart liquids, depending on their composition and application. Various additives play an effective role to minimise settling of magnetic particles and to maintain a coating on the particles in MR fluids. Furthermore, some additives can provide enhanced anti-wear, anti-oxidation properties or pH control in MR fluids [11].

2.3.1 Characteristics of MR Fluids

The essential characteristic of MR fluids is the rapid and distinctive reversible transition from the state of a Newtonian-like fluid to the behaviour of a stiff semi-solid by applying a magnetic field. This characteristic, called the magnetorheological effect, can be understood from the fact that the particles form chain-like structures aligned in field direction. In the absence of an external magnetic field, MR fluids have a relatively small viscosity due to no net magnetisation exists within the particles. When a magnetic field is applied, the flow resistance of the fluid is intensified because of the particles are polarized and align in the field direction to form chains, column or more complex structures. As a result, the MR fluid exhibit solid-like behaviour with increased shear-yield stress. Typical maximal yield shear stress values of state of the art MR Fluids exhibit 50-100 kPa [2,7,11]. Interestingly, once the magnetic field is removed, MR fluids return back to their original 'off' state within milliseconds. By adjusting the magnitude of the applied magnetic field, the transition of solid-liquid state can be precisely and proportionally controlled. Therefore, these characteristics provide concurrent and synchronized response interfaces between electronic control and mechanical systems.

The strength of the yield shear stress is dependent on several factors such as particle size, volume fraction, magnetic field force and type of carrier fluid [3]. For example, both larger particle size and higher volume particle fraction leading to a rise of the yield shear stress value. Higher particles fraction can be achieved by mixing two different particle sizes. Similarly, the value of the yield stress also increases as the magnetic field increases [2,3,11]. It is also believed that in addition to magnetic interactions between two particles, the structure of the particles contribute to a certain level to the enhancement in the apparent viscosity [7].

MR fluid effect is often characterized by Bingham Plastic model, which describes the field-dependent behaviour of MR fluids [17]. In the absence of a magnetic field, MR fluid behaves as a Newtonian fluid. However, in the presence of a magnetic field, a yield stress develops and the fluid behaves as a Bingham fluid. The Bingham constitutive relation can be written as

$$\tau = \pm\tau_0 + \mu\frac{du}{dy} \qquad (2\text{-}1)$$

where τ_0 is the field dependent yield stress, μ is the viscosity, and du/dy is the shear rate [17]. The Bingham plastic model is illustrated in figure 2.5, which is effective in representing the field dependent behaviour of the yield stress of an MR Fluid.
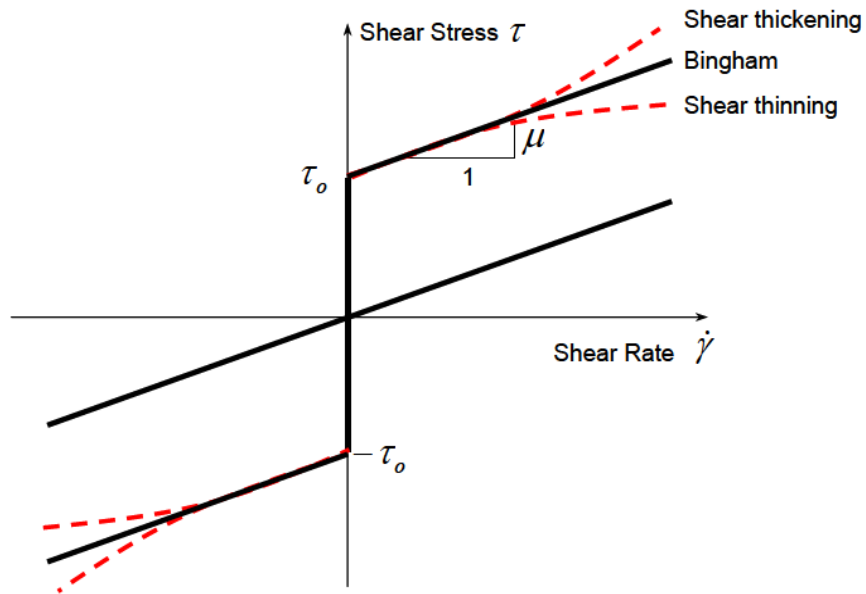
Figure 2.5. Bingham Plastic Model often used to describe MR fluids.
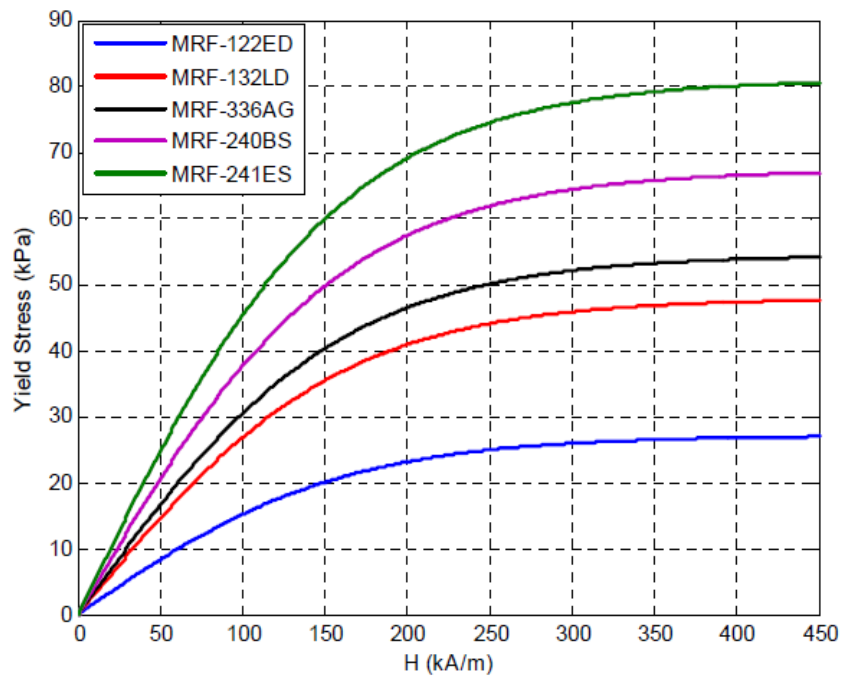
Figure 2.6. Predicted yield stress as a function of applied field [12].

Another essential relationship regarding MR fluids characteristic is the yield stress as a function of applied field strength. It is well known that the yield stress developed in the

fluid increases proportionally with increasing magnetic field strength [18]. The yield stress continues to increase until the fluid reaches magnetic saturation. Figure 2.6 shows the predicted yield stress as a function of applied field for several MR fluids available from Lord Corporation. This model assumes that the yield stress will be developed, regardless of the operating conditions of the fluid [18].

2.3.2 MR Fluids Modes of Operation

Basically, for most industrial applications and devices, the use of smart materials has been divided into three modes of operation or any combination of these three depending on the function of the system. These modes of operation are identified as valve (flow) mode, shear mode and squeeze mode [1,11,13]. MR fluid devices use at least one of the three basic modes of operation of MR fluids. Before designing an MR fluid device, the modes of operation and other elements such as the rheological properties of MR fluids, minimum volume of active MR fluid, the design of the magnetic circuit and electrical power requirement should be cautiously taken into account due to they may influence the properties of the MR fluid device [13].

a)   *Valve mode*

The first mode of operation is valve mode. In this mode, the MR fluid is made to flow between static plates by a pressure drop, thus the flow resistance can be controlled by the magnetic field which is applied perpendicular to the flow direction [1,13], as shown schematically in figure 2.7(a). As a result, the increase in yield stress or viscosity changes the velocity profile of the MR fluids. Examples of the valve mode application include servo valves, dampers, shock absorbers and actuators which could be applied in some devices such as vibration dampers, active engine mounts, knee prosthesis, propshaft mounts and seismic dampers for civil industry [11,13].
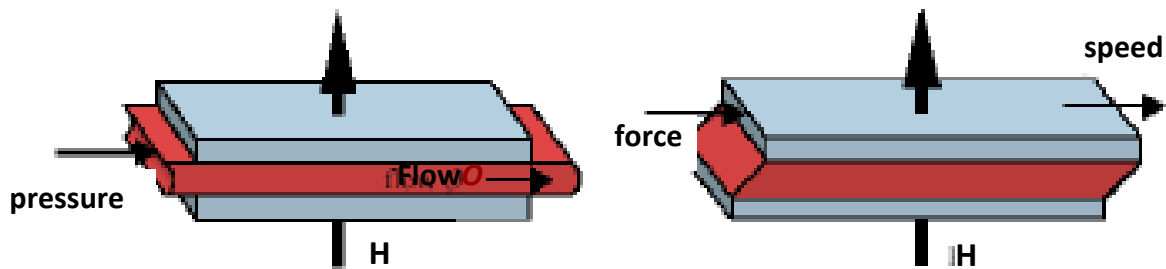
Figure 2.7. MR fluids modes of operation for (a) valve mode and (b) shear mode [12].

b)   *Shear mode*

The second mode of operation is one that allows relative motion between the surfaces moving either in translation or in rotation with the magnetic field applied perpendicularly to the direction of motion of these shear surfaces, as illustrated in figure 2.7(b). This type of

relative motion causes shear in the MR fluid and is thus referred to as the shear mode. The characteristic of shear stress versus shear rate can be controlled by the magnetic field; therefore a Bingham plastic fluid can be represented the behaviour of the MR fluid in this mode [17]. MR fluids technology appropriate for various applications due to their distinctive characteristics of the shear mode such as rapid response and simple interface between electrical power input and mechanical power output using magnetic fields. Examples of the shear mode application include clutches, brakes, chucking and locking devices, dampers, polishing devices and structural composites [6,13].

c)   *Squeeze mode*

The final mode and the one of concern in this study is the squeeze mode. In this mode, an MR fluid is compressed between two parallel plates and thus squeezed out radially [4,19]. The plates are free to move in a direction parallel to the applied field, resulting in placing the MR fluid in tension and compression, as illustrated in figure 2.8. As the plates move toward each other they squeeze the MR fluids, causing it to escape from the perimeter. In the 'on' state, the iron particles line up in the direction of the magnetic field and form chain-like structures, consequently increase the resistance of MR fluids to flow. The flow resistance in squeeze mode is greater than in shear mode. The reason for this is because in shear mode, these chains break and reform continuously, however in squeeze mode, the chains break and form shorter and thicker chains, which are more difficult to break [13,19]. Commercial applications of the squeeze mode so far restricted to small-amplitude vibration control, impact dampers, haptic devices and MR fluid-elastomeric vibration isolators [1,4,13].

Figure 2.8. MR fluids mode of operation: Squeeze Mode

d)   *Multi-mode*

In order to achieve greater performance and functionality, some applications of field responsive fluids use a combination of the three modes of operations. The benefit by applying this approach is to take advantages from each mode, extent their limitations and finally optimise them to gain the best outcome. Example of this application is dampers, which can be constructed in three different modes. It has been proved that the combination

of them gives higher yield stress and produces higher passive damping as compared to any individual mode of operation [3,6].

2.4   Microstructure Study of MR Fluids

MR fluids have already proved their capability in various industrial sectors, particularly in the last decade. However, there are lot of MR based devices require stronger MR fluids for their applications. For instance, the available strength of MR fluids is not satisfactory for manufacturing flexible fixture and automobile clutches [20,22]. For that reason, efforts to improve the strength and capability of MR fluids must be taken.

In order to enhance the durability of MR fluids, it is very crucial to investigate and improve the microstructure of MR fluids [20,21]. For example, Tao et al. employed a rapid compression-assisted-aggregation process to force iron-based MR fluids at a moderate magnetic field of B = 0.576 T. The results were very impressive where the structure-enhanced yield shear stress exceeded 800 kPa, notably ten times stronger than the single-chain microstructure [20-21].

2.4.1   Microstructure of MF Fluids

MR fluids have been proved to hold the same microstructures as in the ER fluids [20,21]. Without the application of magnetic field, the conventional microstructure formation in MR fluids is established by the field-induced polarization, similarly to ER fluids. Tao et al. [20,21] have used computer simulation to describe the chronological movement of the particles in the MR fluids in 'off' state and after a magnetic field is applied, as illustrated in figure 2.9.

From the simulation, the formation of a conventional MR microstructure can be divided into two developmental stages. The first stage involves the chain formation, which only takes few milliseconds to accomplish after a magnetic field is turned on. At this early stage, the fluid already has a yield shear stress and its effective viscosity is drastically increased. However, the formed chains are still uneven and the microstructure has almost no lateral ordering [20]. The second stage is involving the development of the microstructure into a three-dimensional (3D) ordering structure and aggregation of chains into the formation of thick columns that appear as crystalline structure, which relatively is slow process. This process may takes in minutes if the MR system is larger and more complex [20,21].
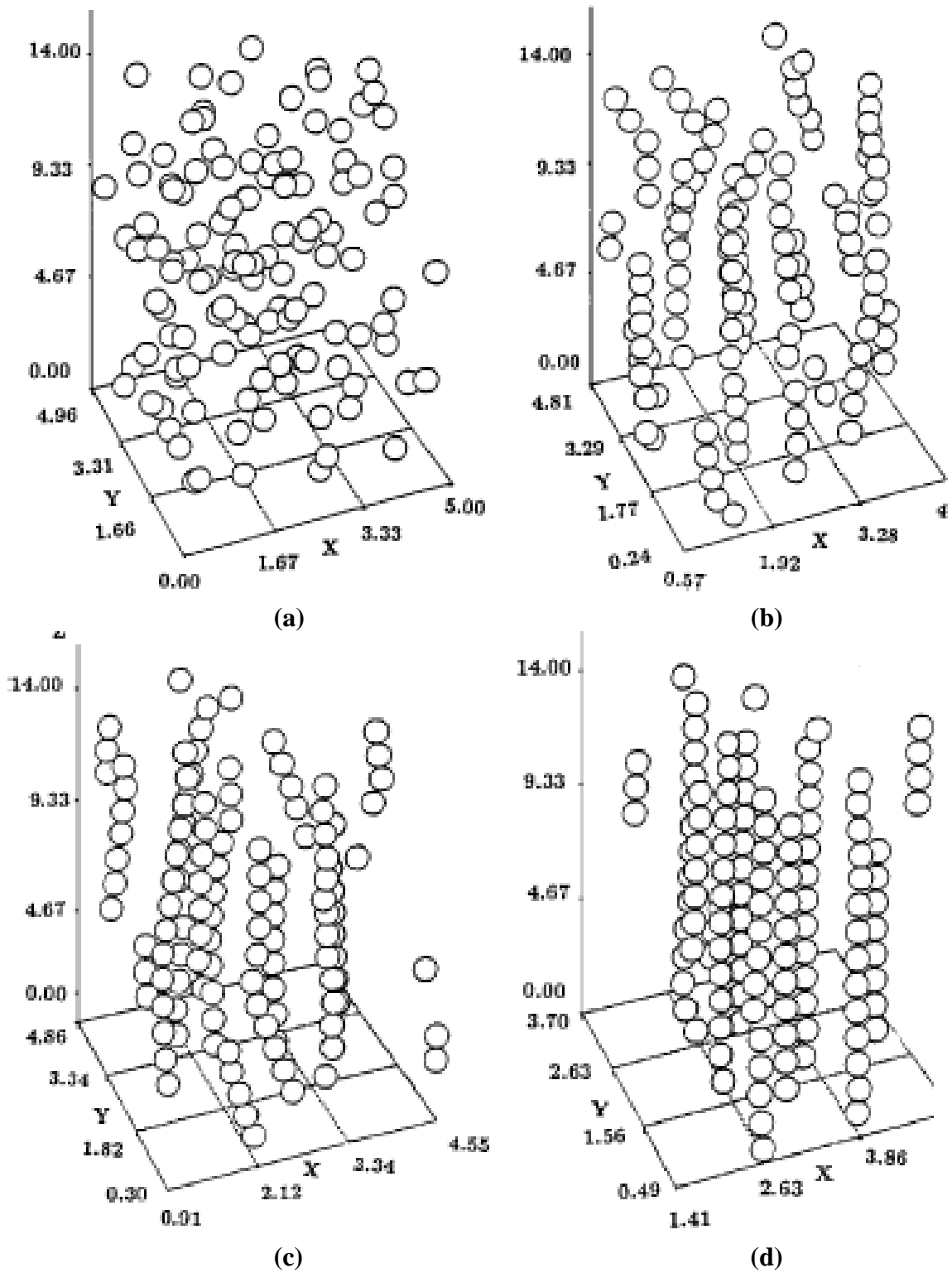
Figure 2.9. Simulation of MR fluids microstructure: (a) 'off' state, (b) 'on' state, t = 10ms, (c) chains become straighter, t = 0.5s, and (d) chain aggregate to form thick column, t = 2.2s [20].

The knowledge of the microstructure and rheological properties of the MR fluids including their weak points is very crucial in order to develop MR fluids with higher durability. With the comprehensive understanding, effort can be worked out to enrich and strengthen the fluids. Tao and co-workers found that one of the weak points of the MR fluids is the breaking point of particle chains [20-22]. When applying an external shear force on the single-chain structure, they found that the chain deformed, became slanted, and eventually broke into two broken chains after the shear force exceeded the threshold. Since the system is symmetry, conventional wisdom predicts that the chain could break at the middle. In contrast, the fact was the breaking point occurred at either end of the chains. They explained that the phenomenon occurred due to the formation process of a long chain along the field direction is energetically favoured, thus the configuration with the minimum energy became unstable and no longer symmetric under such a deformation. As a result, a gap appeared at one end of the single-chain structure during the initial deformation [20,21].

2.4.2   Visualization Techniques

Basically, all visualization techniques use radiation to gather information from samples. In specific, the radiation interacts with the sample and results a measure of the material's composition. The various visualization techniques are classified by the type of radiation as well as by the interaction between them [23]. In the next following text, two visualisation techniques for the purpose of the investigation of the MR fluids microstructure will be discussed.

a)   *Optical microscopy*

Essentially, the optical microscopy works by illuminating the sample with visible light in order to subdivide optical microscopes. As a result, an optical lens train magnifies the image. These techniques can be categorized into transmission, reflection and confocal microscopy [23]. In transmission microscopy, the essence of this technique is the transmission of light by the targeted sample. In contrast, reflection microscopy as illustrated in figure 2.10, uses the reflection of light on the object to generate an image. Meanwhile, confocal microscopy has a capability of depth-discrimination which means the depth of focus of previous methods can be increased [23].

Figure 2.10. Optical pathway of a reflection microscope [24].

Jansen [24] has done several examinations using these techniques for active and non-active MR fluids (MRF-132AD manufactured by Lord Corporation). He found that, in the case of non-active MR fluids samples, reflection microscopy was more capable to obtain good results. Figure 2.11 shows the image of particles in MRF-132AD that obtained using this technique. The weakness of transmission microscopy was the technique only applicable for very thin samples meanwhile confocal microscopy did not perform much more insight in the MR material.
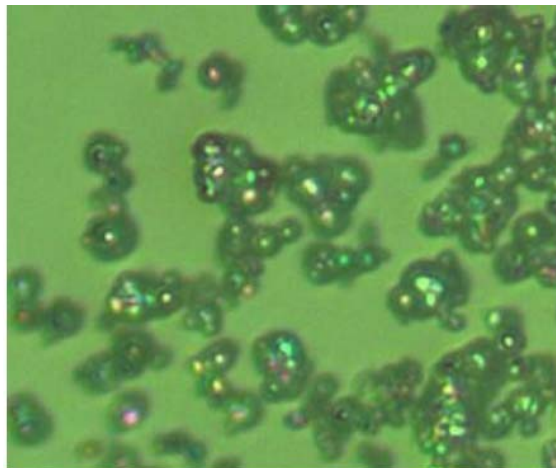
Figure 2.11. Image of MRF-132AD obtained by reflection microscope [24].

b)   *Scanning electron microscopy (SEM)*

Scanning Electron Microscopy (SEM) as shown in figure 2.12 is a technique, which uses a beam of electrons to scan the surface of a sample to build an image of the specimen. When the electron beam hits the sample, the interaction of the beam electrons from the filament and the sample atoms generates a variety of signals including secondary electrons, backscattered electrons, X-rays, light, and even transmitted electrons [23]. Jansen [24] also used this technique to examine non-active MRF-132AD. He found that the images obtained by using the SEM were the best by far, with respect to depth of view and depth of focus (example is shown in figure 2.13).

Figure 2.12. Zeiss EVO scanning electron microscopy (SEM) [25].
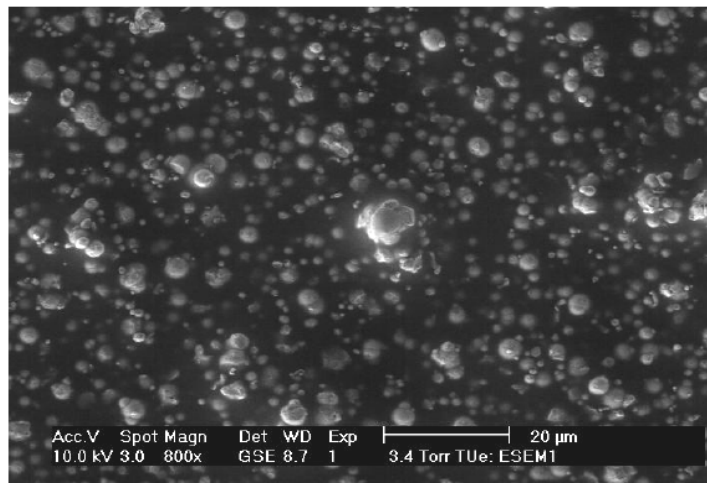
Figure 2.13. SEM image of non-active MRF-132AD [24].

2.5 Applications of MR fluids

After about five decades of research and development, MR fluids began to have commercial applications. Beginning of the commercialization of MR technology was year 1995 and use of rotary brakes in aerobic exercise equipment [11,13]. From this moment application of MR material technology in real-world systems has grown steadily. Nowadays, high-tech MR fluids are becoming predominantly in applications concerning active control of vibrations or torque transfer. For these applications, mode of operation, rheological properties of fluids, design of the magnetic circuit, flux guide and coil configuration are all crucial parameters for the operation of the MR based devices. Since MR fluids are considerably stronger than ER fluids in term of yield stress produced, this makes MR fluids more attention. The MR fluids impact on the automobile industry, building construction, transportation and biomedical engineering is significantly notable. Examples of commercial products of MR fluids such as shock absorbers, vibration dampers, seismic vibration dampers, clutches and seals, linear dampers and MR polishing machines [1,20]. Further, the applications of MR fluids in several industrial sectors will be discussed.

2.5.1 Automotive Industry
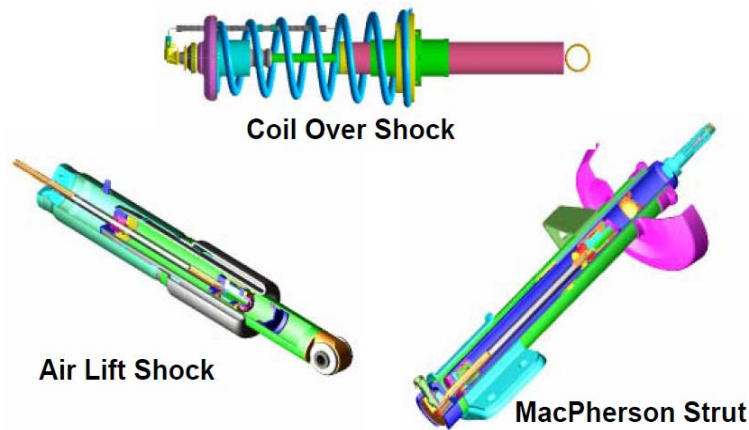
Figure 2.14. Magne-Ride controlled damper configurations [12].

In the marketplace today, automotive-suspension technology is the most productive application of MR fluids. Therefore, considerable effort has gone into the development of dampers using MR fluids. Particularly noteworthy is the development of Magne-Ride^{TM} semi active suspension system, which adjusts damping levels with the combination of MR fluid based struts and shock absorbers, developed by Delphi Automotive Systems and Cadillac. They use materials supplied by Lord Corporation and supply the Magne-Ride^{TM} systems to automotive manufacturers such as General Motors [6,7,26]. The Magne-Ride controlled dampers (figure 2.14) debuted in the 2002 Cadillac Seville STS and 2003 Chevrolet Corvette,

and followed by other models of Cadillac, Chevrolet, Audi, Ferrari and etcetera as illustrated in figure 2.15 [12]. The advantages of using the Magne-Ride[TM] systems include a 40% reduction in mechanical parts, mostly valves, taking away the traditional shock-absorber fluid, and the capability of adapting to changing levels of shock and motion 500 times/s [26].
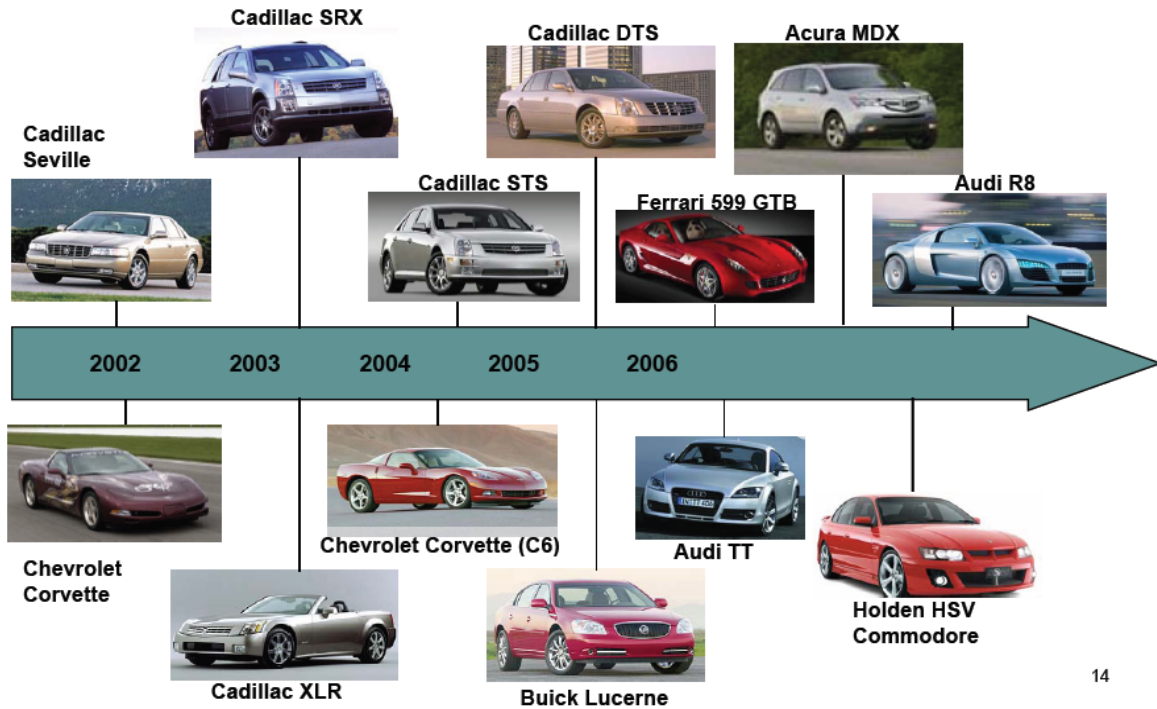
Figure 2.15. Commercial Vehicles Featuring Lord MR Technology in the Delphi Magne-Ride System [12].

Other automotive applications of MR fluids that are of interest are related to the area of steer-by-wire. Steer-by-wire as described in the steering system in figure 2.16 means that there is no mechanical connection exists between the steering wheel and the drive wheels. Replacing mechanical and hydraulic components with simple wire connections enables the vehicle weight to be reduced. This technology is also applied to marine industry and can be extended to brake-by wire, clutch-by-wire, and shift-by-wire in the near years [6,11]. Furthermore, the commercial applications of MR fluids in automotive sector including heavy-duty vehicle seat suspensions, rotary brakes and vibration dampers [7].
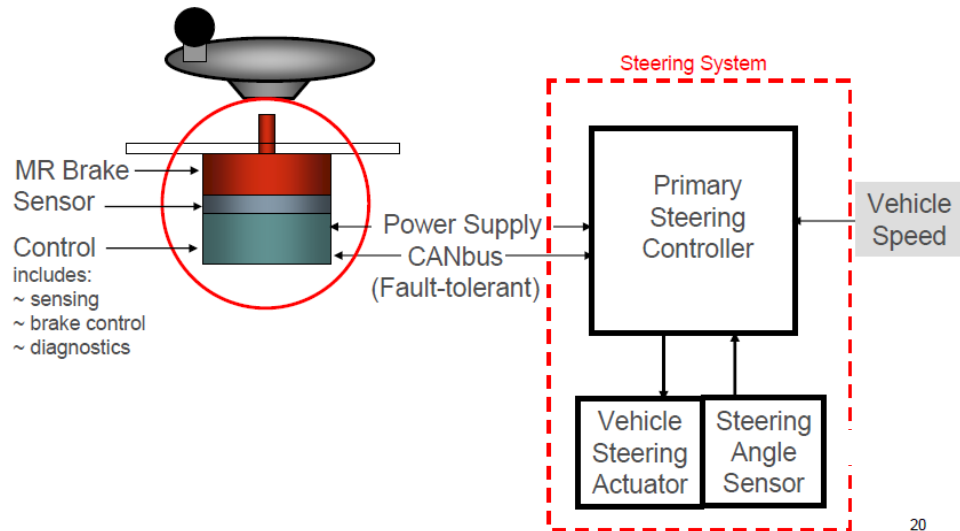
Figure 2.16. Steer-by-wire in the steering system [12].

2.5.2 Civil Engineering Structural Systems

The earliest full-scale implementation of MR dampers for civil engineering applications was realized in 2000. Japanese engineers in Sanwa Tekki installed MRF damping technology (example is shown in figure 2.17) between the third and fifth floors of Nihon-Kagaku-Miraikan, the Tokyo National Museum of Emerging Science and Innovation to help stabilize the building against earthquakes [26,27]. Meanwhile, China constitutes the first full-scale implementation of MR dampers for bridge structures at the Dong Ting Lake Bridge in Hunan. By the technology, the diagonal cables of the bridge are kept steady in bad weather conditions particularly high winds combined with rain that may cause cable galloping [26,27].
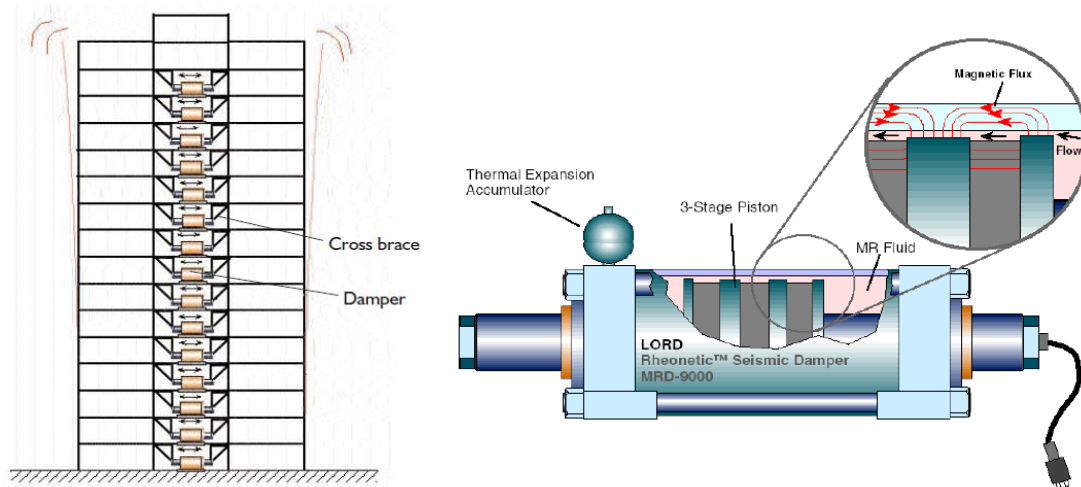
Figure 2.17. Schematic of Lord's 180 kN seismic damper [12].

The application of MR materials in seismic-isolation systems exhibits the reduction of the displacement of structures during near-field earthquakes. As a result, much greater pulsed ground tremors are generated than average earthquakes, particularly close to the epicenter-movements [26]. For a long-term period, the costly investment to implement MR fluids damping systems for critical structures such as hospitals and major data centres would prove worthwhile since a large number of non-MRF isolation systems may not accommodate them.

2.5.3   Biomedical Engineering

Another extraordinary application of MR fluids is real-time controlled dampers in advanced prosthetic devices. In Schwenningen, Germany, Biedermann Motech GmbH has developed its Smart Magnetix prosthetic knee in collaboration with Lord Corporation and introduced its in the year 2000 [18,26]. Smart Magnetix as illustrated in figure 2.18 is a mechanical assembly that consists of a hydraulic piston-cylinder damping component with an electromagnet to stimulate the MR fluid when required. Various sensors are assembled in order to determine the position of the knee and to measure the amount of electrical current that required to be applied to the MR fluids. Interestingly, the artificial device automatically adapts in real time to the user's walking speed and to stairs, slope of terrain, and controls in temperature in a friendly manner [12,26].
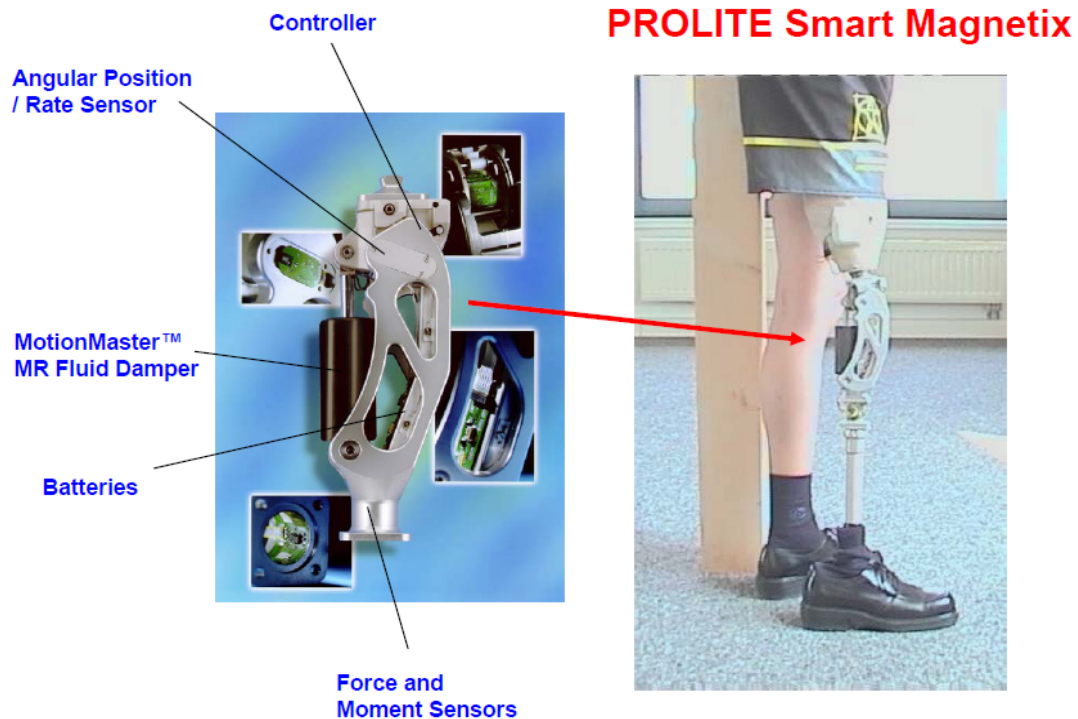
Figure 2.18. Prolite smart magnetix [12].

2.5.4   Fluids for the Future

From an engineering viewpoint, the durability and control issues of MR fluids and MR devices have remain a major challenge in the future. For example, MR fluids clumping and settling problems, shearing stress cycles and also fluctuation temperature performance of over extended periods of time are a big concern [6,26]. Even though the clumping and settling problems could be overcome with the supplement of additives that keep particles suspended, yet advanced research about the fundamental principles behind the clumping phenomenon could lead to better solutions. The challenge is that space is the best place to investigate the problems in, where the clumping pattern is not distorted by the gravity [26].

Various non-technical aspects associated to MR technology are also important challenges. For example, most of MR fluid based devices require a specially formulated MR fluid because of their uniqueness and functionality. As a result, mixing and handling the material on a large scale will be a big issue [26]. Moreover, the number of global manufacturers of high quality iron powders is very small and consequently the available powders are relatively expensive, even in larger scale quantities [6]. Therefore, an increased availability of high quality MR products from different manufacturers and a closer relation between the manufacturers, suppliers of raw materials and MR device manufactures hopefully will be advantageous in increasing the assortment and quantity of commercial applications of these smart materials.

It is tremendous hopes that more advanced industrial applications of the MR fluids will be finally appear on the horizon of the technological landscape in the near future. Few years ago, American scientists have been doing continuous research works on how to control the flow of blood to cancerous tumour by injecting biocompatible MR fluids directly into the bloodstream [26]. In the robotics manufacturing, someday MR fluids might flow in the veins of robots to animate their hands and limbs as naturally as those of humans, or provide active handgrips that match to the profile of each individual hand or fingers. Other promising applications of MR technology in the future include shock absorbers for payloads in spacecraft and producing magneto-liquid-mirror telescopes that bend and deform to cancel out the twinkling of starlight in order to allow the astronomers to achieve better observations [26].

CHAPTER 3

EXPERIMENTAL PROCEDURES

3.1   Introduction

Microstructure study of MR fluids is very crucial in order to find the opportunities to strengthen the performance and durability of the MR fluids. For that reason, it is essential to visualize the microstructure of the MR fluids to obtain a better insight in the fluid. In this project, scanning electron microscopy (SEM) technique was used. Epoxy was chosen as the carrier fluid as well as solidification agent to mix with Carbonyl Iron Particles (CS) at 10% and 20% volume fraction. Since the samples need to be prepared in 'on' state and under compression, the solidification processes were run in line with the compression tests. Several processes were conducted to the cured samples such as mounting, polishing, and gold coating, in order to prepare the SEM specimens. Finally, SEM examination was conducted and the captured image were analysed.

3.2   Material Preparation

Carbonyl iron based suspensions are well known of their good performance and widely used in magnetic devices such as dampers; therefore it seemed interesting to study them. In this project, Carbonyl Iron Particle was chosen because of its high magnetic permeability and low coercivity. Furthermore, the microstructure of these particles could be easily observed and analysed by SEM. In order to prepare SEM specimens in the final stage of this project, Epoxy was selected as solidification agent as well as the carrier fluid. This kind of polymer has curing time about two hours. Therefore, the actual solidification time of the mixture of the CIP and Epoxy needed to be examined.

3.2.1   Composition

In this project, Carbonyl Iron Powder (CIP) was selected as a model particle suspended system. This was because carbonyl iron was magnetically soft material and characterize by high saturation magnetization. The synthesis of CIP from a chemically produced, highly purified intermediate was the reason for its high purity and unique morphology. CIP was produced by thermal decomposition of iron pentacarbonyl ($Fe(CO)_5$), which was previously distilled to high purity [16]. The average particle size and tap density were 1.0-8.0 μm and 7.8 g/cm^3, respectively. The unique properties of CIP were spherical particle structure, full density particles, low metal impurities, high chemical purity grades with iron content up to 99.8% available, and excellent lot-to-lot consistency [16].

The primary function of a carrier liquid was to provide a liquid in which the magnetically active phase particulates were suspended. Accordingly, the carrier liquid should also be largely non-reactive towards the magnetic particles. In this project, Buehler Epoxy which consisted of Epo-Kwick resin and hardener was selected as the carrier fluids as well as

curing agent. This epoxy was chosen due to the fact that in the process of polymerization of the resin, the phase transformations occur sufficiently slowly. The mixed ratio of the epoxy was five parts of epoxy resin to one part of epoxy hardener. It was essential that this correct mixed ratio be obtained between them to ensure that a complete reaction took place. Otherwise, the final properties will be affected due to the un-reacted resin or hardener.

3.2.2 Viscosity Test

Before the SEM samples were prepared, it was necessary to examine the rheological behaviour of the epoxy and the mixture of CIP and epoxy. In another word, viscosity test might be conducted separately to observe the viscosity change of both fluids before they became completely cured. For this purpose, a universal dynamic viscometer as shown in figure 3.1 was used to carry out the experiments. All viscosity tests were conducted at room temperature.

Figure 3.1. Universal dynamic viscometer.

In this experiment, three samples with different volume as shown in table 3.1 were tested. The first sample was epoxy solely and was set as a benchmark for two other samples. The mixed ratio was fixed to 5 parts of resin to 1 parts of harder, as guided by the manufacturer (Buehler).

25

Table 3.1. Samples of viscosity test.

No.	Samples	Epoxy Resin (ml)	Hardener (ml)	CIP (ml)
1	Epoxy (Resin + Hardener)	5	1	-
2	Epoxy + 10% CIP	5	1	0.67 (~5.3g)
3	Epoxy + 20% CIP	5	1	1.5 (~11.7g)

The two other samples were the MR fluids models with 10% and 20% volume fraction of CIP. The percentage of volume fraction could be simply calculated by this formula

$$\%CIP = \frac{Volume\ of\ CIP}{Volume\ of\ CIP,\ resin\ and\ hardener} \qquad (3.1)$$

Therefore, in order to prepare 10% volume fraction of CIP, 0.67 ml CIP was required to be mixed with 5 ml of resin and 1 ml of hardener. This amount of CIP was prepared by calculating the equivalent weight by simply multiple the volumes by the CIP density, which was 7.8 g/cm^3, thus the required weight of CIP was 5.3g for 10% volume fraction. Correspondingly, an amount of 1.5 ml or 11.7g of CIP was required to prepare the 20% volume fraction. The weight of CIP for these two samples was measured accurately by Kern's electronic scale.

For the first sample, 5 ml of epoxy resin was prepared by using pipette and poured into a disposable paper cup. 1 ml epoxy hardener also prepared by pipette mixed with the resin and immediately a stopwatch was started. The mixture was blended gently but thoroughly for about two minutes by using stirring stick. Subsequently, a spatula took a small amount of the fluids and put onto the base of the viscometer and was spread. The viscosity of the epoxy was recorded for every five minutes, until the value of viscosity considerably very high and no more significant. For the two remaining samples, the epoxy were mixed and blended thoroughly with the CIP, before added the hardener. After that, the same processes as in the first experiment were followed.

3.2.3   Sample Preparation

As the preparation for the next two important experiments, the mixtures of CIP for both volume fraction and epoxy resin were prepared sufficiently in larger amount. Meanwhile, the hardener couldn't be mixed earlier and only be prepared prior to every individual test. It was calculated that the amount of MR fluids model required for each 10% and 20% volume fraction of CIP for the whole experiments was about 100 ml. Therefore, the required amount of CIP, epoxy resin and hardener to prepare the compounds were calculated and are shown in table 3.2 (for 10% volume fraction) and table 3.3 (for 20% volume fraction).

Table 3.2. The amount of CIP, Epoxy resin and hardener required for the whole experiment for 10% volume fraction of CIP.

Parameters	Unit	CIP	Resin	Hardener
Volume (individual test)	ml	0.67	5	1
Percentage	%	10	75	15
Volume required	ml	10.0	75.0	15.0
Weight of required CIP = 10 ml x 7.8 g/cm^3 = 78 gram				

Table 3.3. The amount of CIP, Epoxy resin and hardener required for the whole experiment for 20% volume fraction of CIP.

Parameters	Unit	CIP	Resin	Hardener
Volume (individual test)	ml	1.5	5	1
Percentage	%	20	66.67	13.33
Volume required	ml	22.5	75.0	15.0
Weight of required CIP = 22.50 ml x 7.8 g/cm^3 = 175.5 gram				

For sample of 10% volume fraction, an amount of 78 gram of CIP was mixed with 75 ml of epoxy resin in a plastic laboratory bottle. Subsequently, the mixture was blended together by using electric stirrer for about half an hour. Accordingly, an amount of 175.5 gram of CIP was mixed and stirred together thoroughly with 75 ml of epoxy resin as per sample for 20% volume fraction. These compounds were used in the next experiments, where the mixture was required to be remixed.

3.3   Compression Tests and Solidification Process

In this experiment, a number of compression tests were conducted. There were two main purposes of the compression tests. The first purpose was to investigate the stress-strain relationships of the materials and second was to prepare the SEM specimens. After each compression test was complete, the value of applied magnetic field was kept constant for about 3 hours in order to allow the curing process occurred completely.

3.3.1 Remixing the Compounds

The MR fluids compounds were remixed prior to all individual compression tests. The suspensions were homogenized by the agitation of an electrical stirrer at 500 rpm for 15 minutes until the MR fluids achieved a uniform condition. The purpose of this action was to ensure the iron particles redisperse homogeneously in the suspension. Immediately after the remixing of the compound accomplished, the sample required for each individual compression test was prepared. The volume of composition of CIP, epoxy resin and hardener for the each sample were 4 ml and 6 ml for corresponding 10 % and 20% volume fraction, respectively. The detail of the composition is shown in table 3.4 (for 10% volume fraction) and table 3.5 (for 20% volume fraction).

Table 3.4. The volume of CIP, Epoxy resin and hardener required for each individual compression test for 10% volume fraction of CIP.

Parameters	CIP	Resin	Hardener	Total
Percentage (%)	10	75	15	**100**
Volume required (ml)	3.4		0.6	**4**

Table 3.5. The volume of CIP, Epoxy resin and hardener required for each individual compression test for 20% volume fraction of CIP.

Parameters	CIP	Resin	Hardener	Total
Percentage (%)	20	66.7	13.3	**100**
Volume required (ml)	5.2		0.8	**6**

In order to prepare 4 ml of 10% volume fraction sample, the required volume of the CIP and epoxy resin compound was 3.4 ml. This volume was taken accurately by using pipette and pour properly into a plastic laboratory cup. Instantaneously, a volume of 0.6 ml of epoxy hardener was also prepared by using pipette and dispense slowly into the compound. Without delay, the mixture was stirred gently but thoroughly for about 30 minutes by using stirring stick. The purpose for this action was to allow the chemical reaction occurred effectively within the 30 minutes, which was the first phase of the solidification process in the compound. After 30 minutes, the compound was already standing by to be placed in the test rig.

Accordingly, in order to prepare 6 ml of 20% volume fraction sample, the required volume of the CIP and epoxy resin mixture and epoxy hardener were 5.2 ml and 0.8 ml, respectively. The similar procedures were followed but in this case, the sample mixture was stirred for about 40 minutes. The durations of mixing period were figured out in the previous viscosity tests and will be discussed in detail in section 4.2. The different volume of the samples which were 4 ml and 6 ml for 10% and 20% volume fraction, respectively, decided

based on a simple calculation for ease and accurate measurement of the pipette and did not make any sense to the experiments. This was due to only 2 ml from each sample was required to be placed in the test rig.

3.3.2   Compression Tests

Two main objectives of this test were to investigate the stress-strain relationships of the MR fluids under compression mode and simultaneously to prepare SEM specimens in 'on' state and under compression conditions. The already available test rig designed for squeeze mode as shown in figure 3.2 was used in this experiment. The test rig has an upper cylinder with 50 mm in diameter, which was executed to perform the compressive tests [3]. A copper wire coil with 2750 turns and 29 ohms was wound around the lower cylinder to generate magnetic field, which could be controlled by adjusting the supplied current. The advantages of this test rig were it was simple, easy to adjust the working gap (strain) and required only small volume of sample [3].
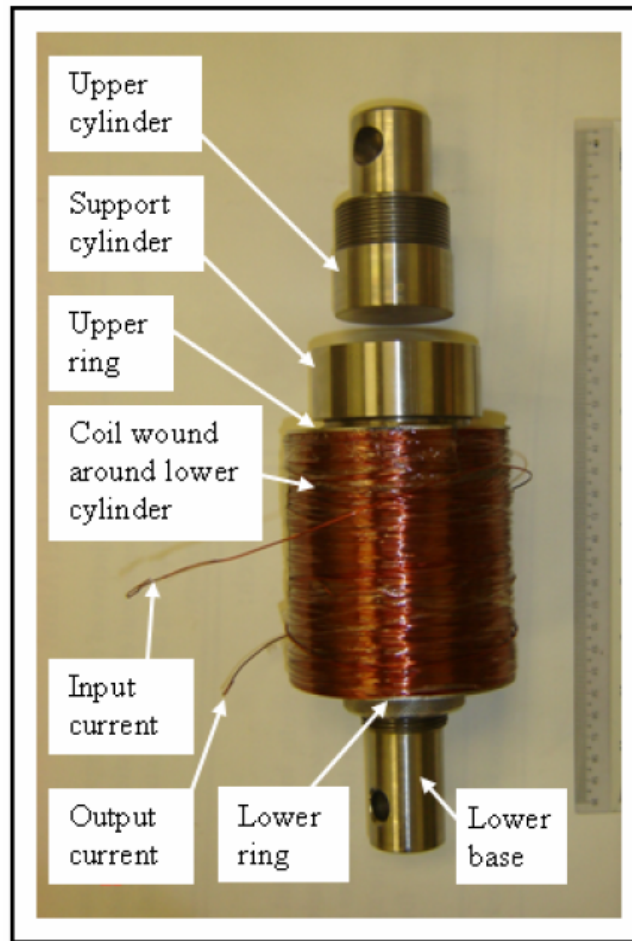

Figure 3.2. Test rig design for squeeze mode [3].

Figure 3.3 shows the schematic diagram of the apparatus of compression tests. Zwick Z50kN Testing Machine was used to perform the compression activities by controlling the displacement between its upper and lower grips. The test rig was installed vertically in the testing machine by fixing it at the lower grips of the testing machine. In order to supply current and generate magnetic field, a DC power supply was connected to the test rig.
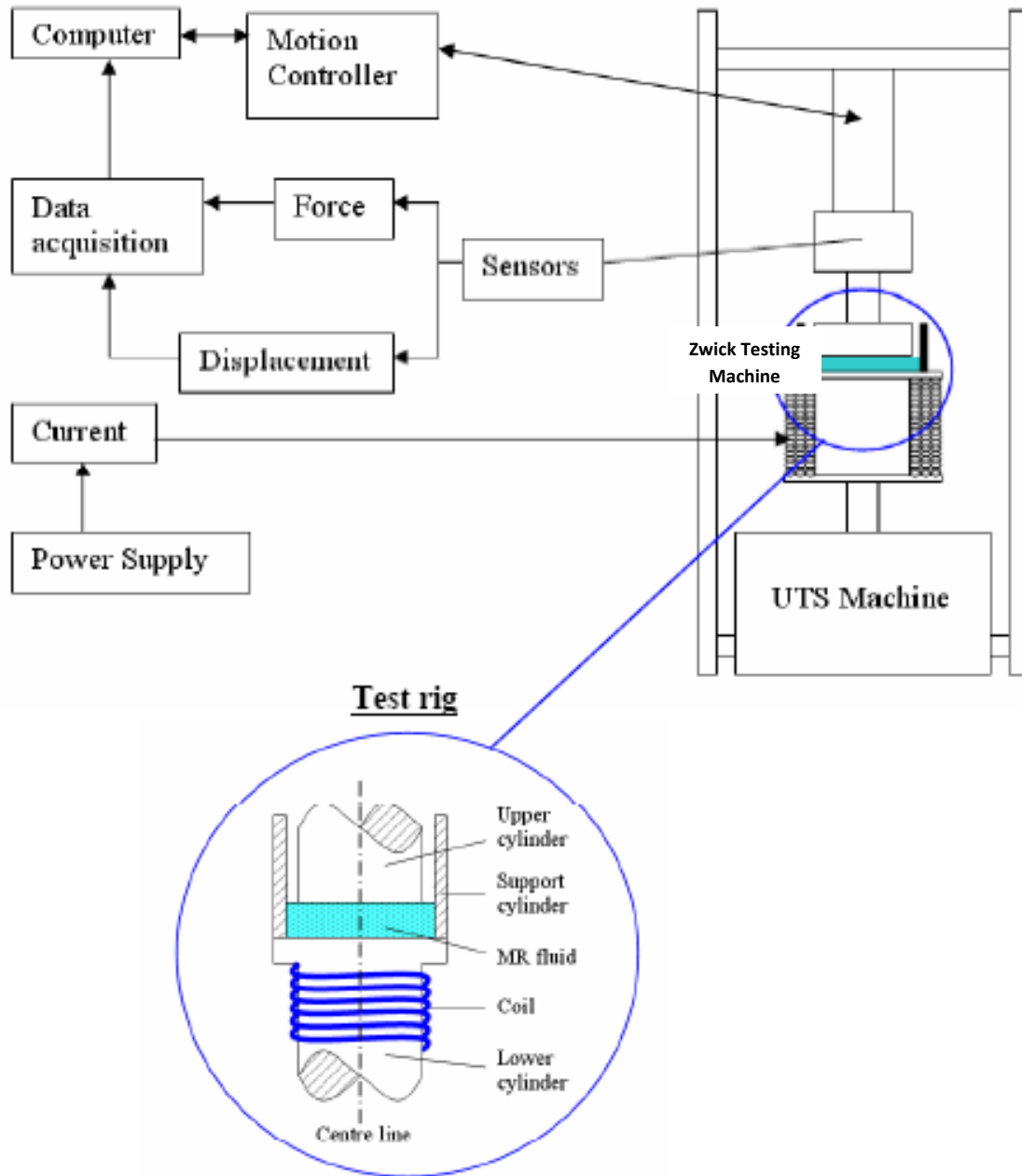

Figure 3.3. Schematic diagram of compression tests [3].

In this experiment, several parameters were fixed to ensure homogeneity for all samples and focus on the compression aspect. For each test, the initial gap was set to 1 mm, therefore, it was calculated that the equivalent volume of sample for this gap was 2 ml [3]. By utilising the Testing Machine's software i.e. TestXpert II, the testing machine was set to execute the tests by a speed of 2 mm/min. Furthermore, for each test, a total of 9 cycles of cyclic test between the initial gaps to a displacement of 0.5 mm was set, followed by compression to the targeted displacement afterwards. The supplied current was set to a constant magnitude of 800 mA, which was calculated to generate a magnetic field of 0.4 Tesla [3]. During the cyclic test, the applied current was turned on throughout compression but turned off when the upper cylinder was returning to the initial gap.

In this experiment, eight tests were conducted as shown in table 3.6. Prior to the test, Buehler release agent were spread onto the upper and lower cylinders of the test rig, in order to take the sample out easily when it was cured. When the testing machine was ready to execute, a volume of 2 ml from the remixed compound as mentioned in section 3.3.1 was transferred cautiously using a syringe onto the centre of the test rig's lower cylinder. Next, the upper cylinder was lowered to the initial gap with a speed of 2 mm/min. Subsequently, the magnetic field was turned on and afterwards, the programme in the software was commenced to perform the compression test. When the upper cylinder eventually reached the targeted displacement, the magnetic field was remained on until about 3 hours.

Table 3.6. Samples for compression tests.

No.	Volume Fraction	Condition	Initial Gap	Final Gap
1	10 %	'On' State	1 mm	1.00 mm
2	10 %	Compression (25%)	1 mm	0.75 mm
3	10 %	Compression (50%)	1 mm	0.50 mm
4	10 %	Compression (75%)	1 mm	0.25 mm
5	20 %	'On' State	1 mm	1.00 mm
6	20 %	Compression (25%)	1 mm	0.75 mm
7	20 %	Compression (50%)	1 mm	0.50 mm
8	20 %	Compression (75%)	1 mm	0.25 mm

As mentioned previously, the solidification process of the samples took place throughout the compression tests. After each compression test accomplished, the samples were left on the test rig for about 3 hours, where the samples were considered completely cured. However, the samples for 'off' state for both volume fractions were prepared separately since no magnetic field and compression test required for these samples. All the samples needed to be prepared prior to the SEM examination and will be explained in the following section.

3.4   SEM Image Analysis

Prior to the SEM examination, all the specimens were prepared cautiously through several processes consisted of cutting, mounting, polishing, coating and finally labelling. The prepared specimens subsequently examined by SEM and three images were captured for each specimen. Finally, all the produced images were analysis by using Image-J software.

3.4.1   Specimens Preparation

All samples produced in the previous experiments were prepared by several processes with regarded to the SEM examination. Initially, each sample was cut into three parts by a diamond saw to produce three specimens which representing top (centre), top (side) and cross-section (side) as described in figure 3.4. The specimens then were mounted by using simplet mounting press, which took about 12 minutes for each specimen. Figure 3.5 shows the specimens that already have been mounted.
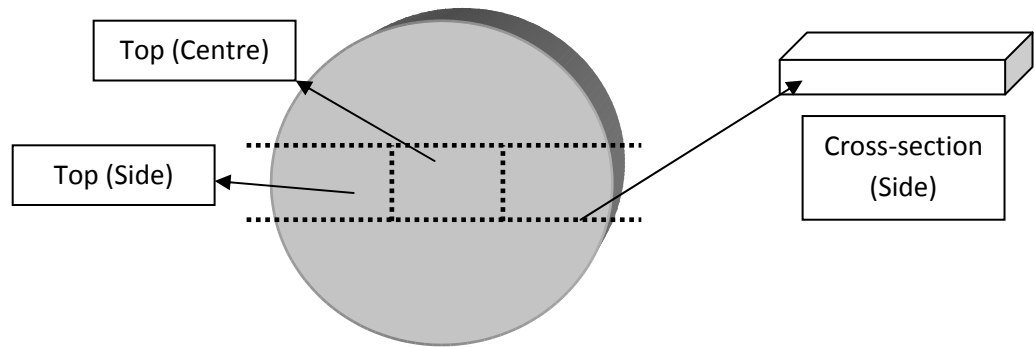

Figure 3.4. Sample cut into 3 specimens.

Figure 3.5. Mounted specimens.

Subsequently, the specimens were polished using Motopol Polishing Machine. The polishing machine was capable to polish six specimens in each individual process. The polishing process conducted using several materials in sequence started with Buehler's Silicon Carbide grinding paper P1200. This process took about 1 minute. Afterwards, the process was continued sequentially with Buehler's diamond suspensions of 9 μm, 6 μm, 3 μm, 1 μm and finally 0.05 μm, which took about 3 minutes for each process. Lubricant was added in the middle of each process to ease the polishing process.

The final process of the specimen preparation was coating. This procedure was to increase their conductivity and mechanical stability as well as to decrease in beam penetration for better spatial resolution results [28]. To do so, scan coater was used. This coater used gold to perform the coating, which has advantages such as high conduction of electrons and heat as well as good granularity of evaporated or sputtered particles [28]. The coating process took about 7 minutes for each specimen. Finally, all the prepared specimens were labelled with identification as shown in table 3.7.

Table 3.7. SEM specimens.

No.	Volume Fraction	Condition	Specimen Labelling		
			Top (Centre)	Top (Side)	Cross-Section (Top)
1	10 %	'OFF'	A	B	C
2	10 %	'ON'	D	E	F
3	10 %	Compression (25%)	G	H	I
4	10 %	Compression (75%)	J	K	L
5	20 %	'OFF'	M	N	O
6	20 %	'ON'	P	Q	R
7	20 %	Compression (25%)	S	T	U
8	20 %	Compression (75%)	V	W	X

3.4.2 SEM Examination

In this stage, the microscopic details of the prepared specimens were examined by using Zeiss Evo Scanning Electron Microscope (SEM) as shown in figure 3.6. The type of signal selected was Back-Scattered Electrons (BSE) on account of the BSE images could provide information about the distribution of different elements in an examined specimen. In principle, BSE consisted of high-energy electrons originating in the electron beam, that were reflected or

back-scattered out of the specimen interaction volume by elastic scattering interactions with specimen atoms [28].
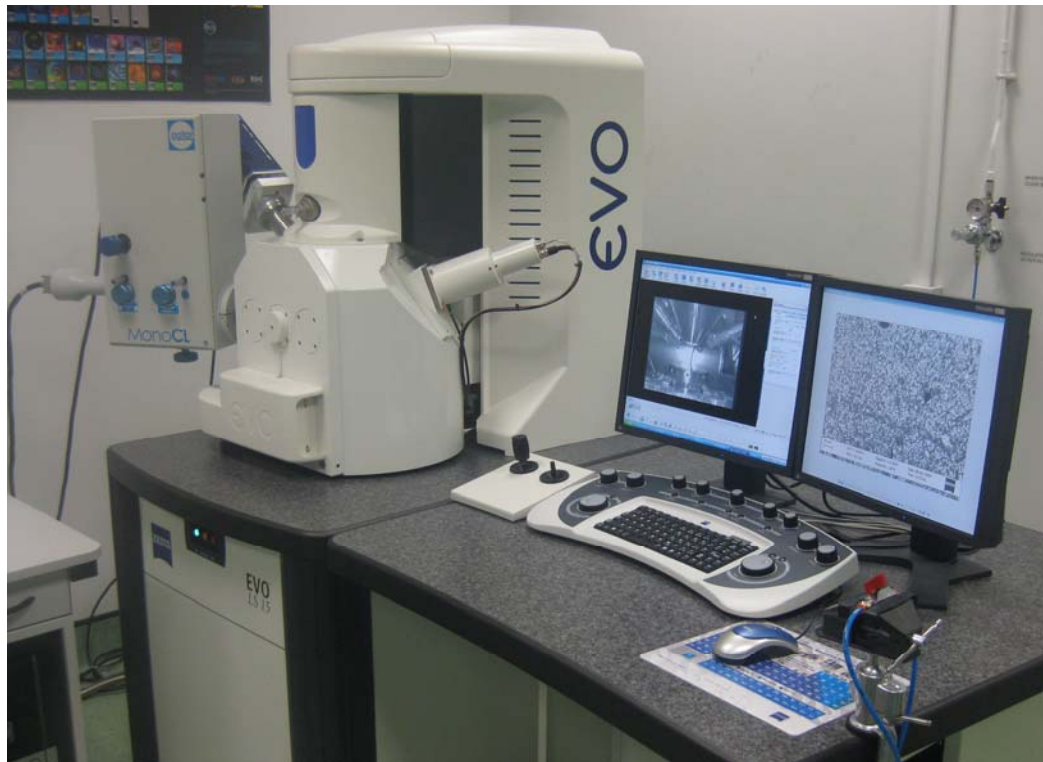

Figure 3.6. Zeiss Evo scanning electron microscope.

In order to conduct the SEM examination, a specimen was firmly attached and held by an electrical tape to the specimen stub inside the SEM. After the SEM was turned on, adjusting the magnification, high voltage set (EHT), Iprobe, contrast and brightness of the SEM, discovered a clear image. For each specimen, three images were captured to represent three magnifications of 400x, 700x and 1000x, thus a total number of 72 images was produced from the 24 specimens. Finally, these images were analysed by using Image-J software in order to investigate the microstructure of the MR fluids in different conditions.

CHAPTER 4

RESULTS AND DISCUSSION

4.1   Introduction

The compression behaviour of MR fluids has been studied extensively for industrial applications such as in dampers and as a method for underpinning the materials by increasing their yield stress [21,29]. For that reason, the scientific aim of this project was to investigate the microstructure of MR fluids in squeeze mode under compression. This chapter first presents with a discussion of the rheological behaviour of suspending epoxy in MR fluids. Next, the stress-strain relationships of the MR fluids, which were obtained from the compression tests were analysed. Finally the microstructures of the MR fluids were investigated by analysing the SEM images. Knowledge of the overall study in this project would contribute towards researching the enhancement of MR fluids.
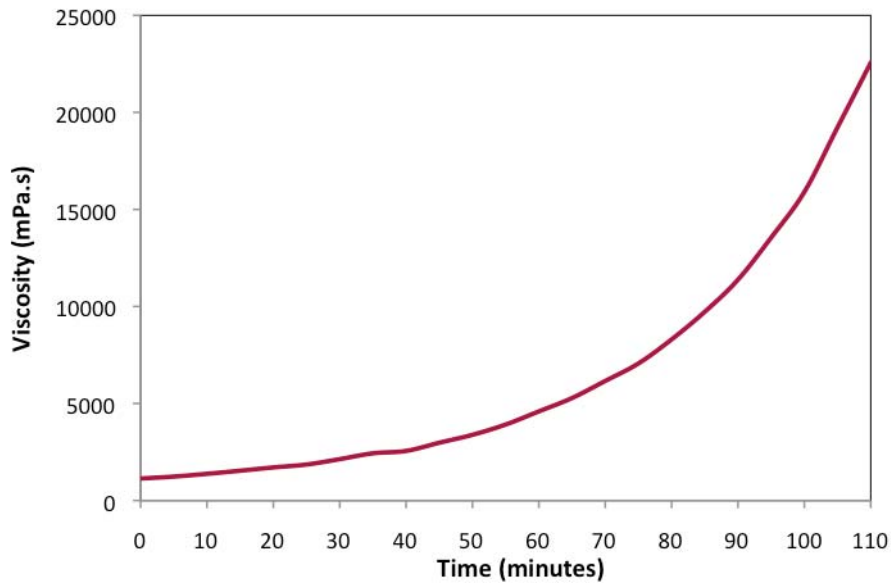
4.2   Rheological Behaviour

Figure 4.1. Viscosity versus Time of Buehler' Epo-Kwick Epoxy.

Figure 4.1 shows the change in viscosity of Buehler' Epo-Kwick Epoxy over time. In normal condition and without adding any other materials, the viscosity of the epoxy mixture showed an exponential increase, once an ample volume of hardener was mixed thoroughly with the epoxy resin. In the first one hour, the viscosity of the mixture increased gradually and reached about 4000 mPa.s. After this point, the viscosity showed an exponential curve and

35

reached over 19,000 mPa.s at 110 minutes. At this point, the mixture was considered as fully solidified.

In order to examine the rheological behaviour of the MR fluids model in this project, viscosity tests of 10% and 20% volume fraction of CIP in epoxy mixture were conducted. The epoxy took part in the compound as the carrier fluid as well as the solidification agent. Figure 4.2 describes the viscosity behaviour of the CIP-epoxy mixtures. In comparison with the neat epoxy mixture (figure 4.1), the viscosities of these epoxy based MR fluids were significantly higher. The viscosities of the mixtures decreased drastically in the first half an hour. After reaching their lowest value, the viscosity started to increase gradually and after about one hour, the viscosity of both mixtures showed an exponential increase in which was similar to the epoxy mixture solely.
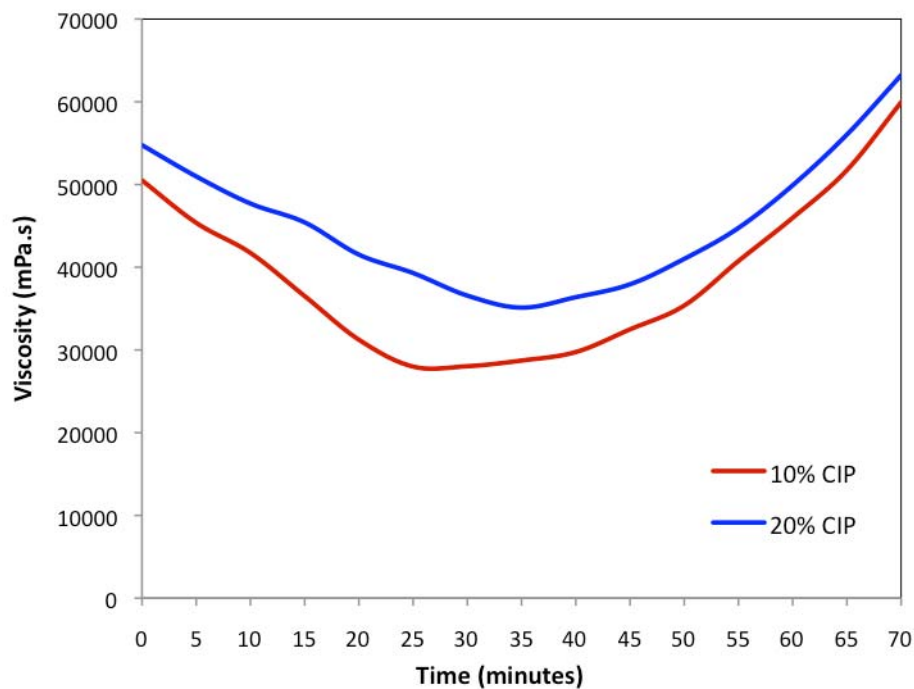

Figure 4.2. Viscosity versus Time of 10% and 20% volume fraction of CIP.

In general, the 10% volume fraction of CIP plotted a similar viscosity curve as the 20% CIP graph, but the viscosities of 20% CIP were always higher. In 10% volume fraction of CIP, the mixture took about 30 minutes to stable before the solidification process started smoothly. Meanwhile, the 20% volume fraction of CIP mixture took 40 minutes in order to stabilize, before the curing process started. These results were very important as the preparation of the compression tests, where the remixing time of the MR fluids was looked at.

Basically, epoxy consisted of two components of short chain polymers that were the resin and the hardener. When the substances were blended together, both materials took placed in a chemical reaction and a covalent bond would be formed, as a result polymer was heavily

cross-linked and eventually became solidified [30]. The chemical reaction is called polymerization process, and normally could be controlled by temperature. The polymerization process involved the binding of single chemical units into long chains. Gradually, these long chains cross-linked to form large networks of interlocking complex three-dimensional structures [30]. As a result, the mixture became completely solid after the solidification time reached.

This fundamental principle explained the exponential increased in the viscosity of the neat epoxy in the experiment. In the early stage of the curing process, since the epoxy resin and hardener just took place in a chemical reaction, the polymerization process focused on the binding of the single units to long chains, for that reason the viscosity level in this period increased gradually. However, after about one hour, the long chains generated large networks of interlocking three-dimensional structures by cross-linking, therefore the viscosity of the epoxy increased drastically before eventually completely cured. On the other hand, the viscosity behaviour of the MR fluids has shown dissimilar appearance in the early stage. The viscosities of the fluids were at high value in the early stage as a result of the increased in density of the compounds due to the addition of CIP. The viscosity of the mixtures then decreased gradually until reaching its lowest value. This situation might because of the polymerization process was progressing slowly in order to stabilise the compounds, after the hardener was added. After about 30 and 40 minutes, respectively the viscosity of 10% and 20% volume fraction of CIP increased drastically in exponential curve, similar as in the second phase of the viscosity in neat epoxy.

4.3   Compression Behaviour of MR Fluids

### 4.3.1   'Off-' and 'On-' State Behaviour

The SEM images at the top (centre) of the specimens for 'off' and 'on' state of the MR fluids in this project is shown in figure 4.3. In addition, the particles distribution on the specimens, which have been analysed by using Image-J software, is shown in table 4.1. This information might help to explain the behaviour of MR fluids before and after the magnetic field was induced. In the 'off' state condition, iron particles inside the MR fluids were dispersed randomly in the suspension since there was no induction of magnetic field. When the magnetic field was induced, the iron particles arrangement in the suspension altered to form chain-like structure.
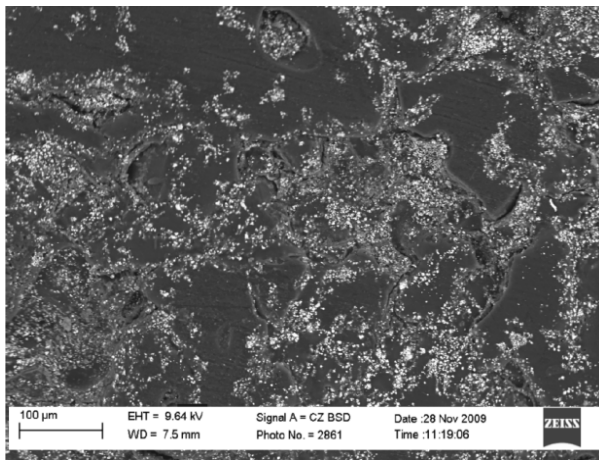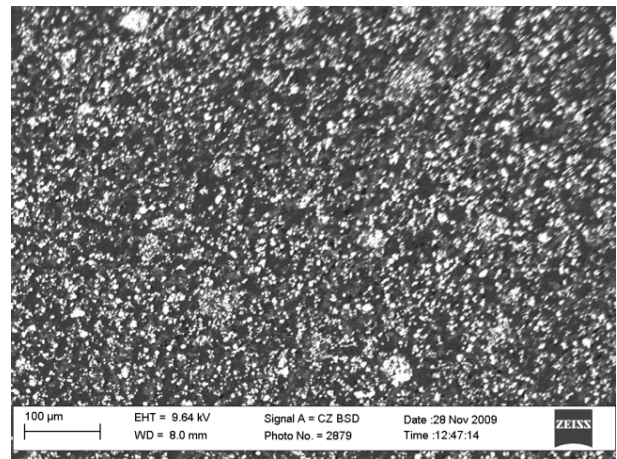
(a)
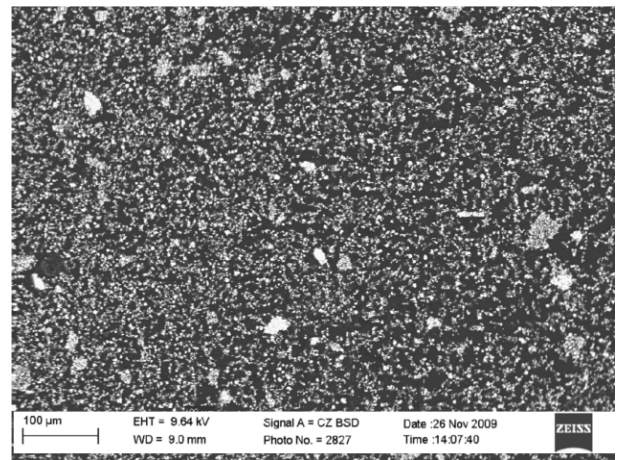
(b)
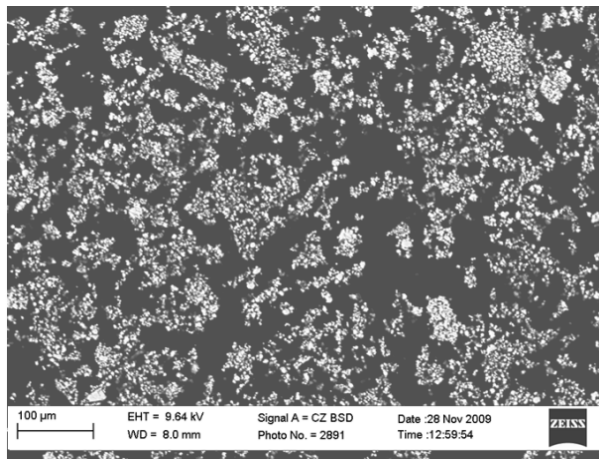
(c)

(d)

Figure 4.3. SEM images (100µm) of top (centre) for (a) 10% CIP - 'off' state, (b) 10% CIP – 'on' state, (c) 20% CIP - 'off' state, and (d) 20% CIP - 'on' state.

Table 4.1. Percentage of iron particle distribution at 'off' and 'on' state.

Volume Fraction of CIP	Specimen	Percentage of CIP Distribution (%)	
		'OFF' state	*'ON' state*
10%	Top (centre)	14.4	17.9
	Top (side)	11.7	17.5
	Cross section (side)	5.0	9.9
20%	Top (centre)	17.6	22.0
	Top (side)	15.8	21.1
	Cross section (side)	14.1	24.1

It can be clearly seen from figure 4.3 that the iron particles' arrangement in 'off' state was not uniform, but randomly on the top of the specimens. In fact, there were some areas of cured epoxy contained not a single iron particle inside. However, the iron particles' arrangements in the 'on' state for both specimens were well distributed. Statistically, the percentage of the iron particles distribution of the specimens in 'on' state was significantly greater than in 'off' state as stated in table 4.1. This information certainly did not mean that the percentage of iron particle in 'on' state was greater than in 'off' state, since the preparation of both samples were used the same amount of volume fraction of CIP. However, the alteration of the particle distribution on the top surface of the specimens was good to describe the distribution of MR fluid in the absence or presence of magnetic field.

The particles distribution on the cross-section and top of the MR fluids before and after a magnetic field was applied perpendicularly can be ideally illustrated in figure 4.4. In 'off' state, since the MR fluid was mixed thoroughly before the curing process, the iron particles dispersed randomly in the epoxy. As a result, the particle distribution on the top surface appeared in scattered as well. In contrast, with the presence of magnetic field, the particle formed chain-like structure in line with the magnetic flux resulting more iron particles appeared on both top and bottom surfaces. For that reason, the percentage of iron particles on the top of specimens was slightly higher in comparison with the absence of magnetic field. However, these results are not the main focus of this study. The knowledge particles distribution is very important as indicators and benchmarks for the investigation of compression behaviour of MR fluids in which will be discussed in the following section.
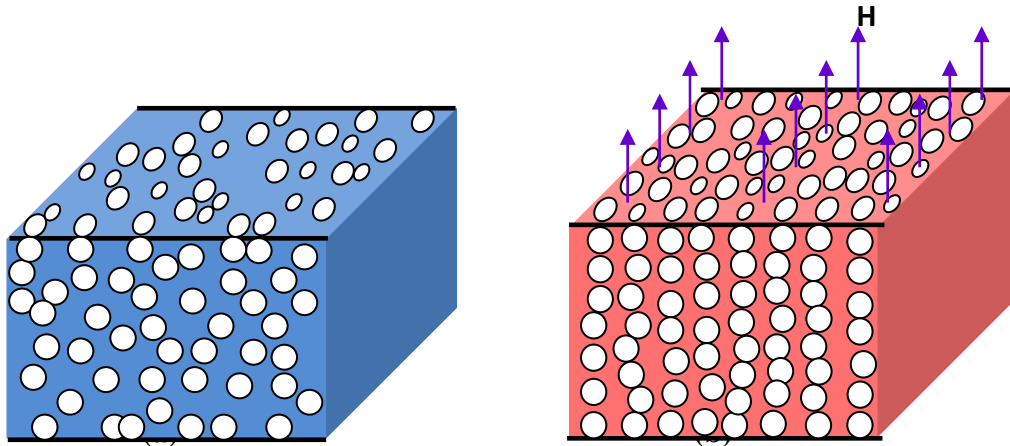

Figure 4.4. Particles distribution in (a) 'off' state and (b) 'on' state.

4.3.2 Compression Behaviour

In this project, three levels of compression tests, given at 25%, 50% and 75% of the compressions have been conducted. In order to emphasis the investigation on the compression behaviour, the other elements such as volume of sample, initial gap distance, speed of upper

cylinder, magnetic field strength and cyclic run were kept constant. Throughout the compression tests, the solidified samples were produced for SEM specimens. In this section the behaviour of the compression of MR fluids will be discussed in more details by analysing the compressive stress-strain relationships and SEM images.

Initially, the behaviour of MR fluids under compressions in term of compressive stress-strain relationship was examined. Figure 4.5 describes the compressive stress versus compressive strain of the MR fluids under compression of 25%, 50% and 75%. From the figure 4.5 (a) and (b), it is clearly shown that the compressive stresses increased drastically at the initial phase of the compression. However the process occurred at the first 0.01 mm of strain or equally 1% of compression. Then, the compressive stresses showed a gradual increased until reaching 0.25 mm of the strain. Interestingly, after 0.25 mm of strain, the compressive stresses increased exponentially until the compression test ended at 0.5 mm and 0.75 mm as shown in figure 4.5 (b) and (c) respectively. The aforementioned behaviour was applicable for both 10% and 20% volume fraction of the MR fluids. However, the compressive stresses of 20% CIP were always higher than 10% CIP.
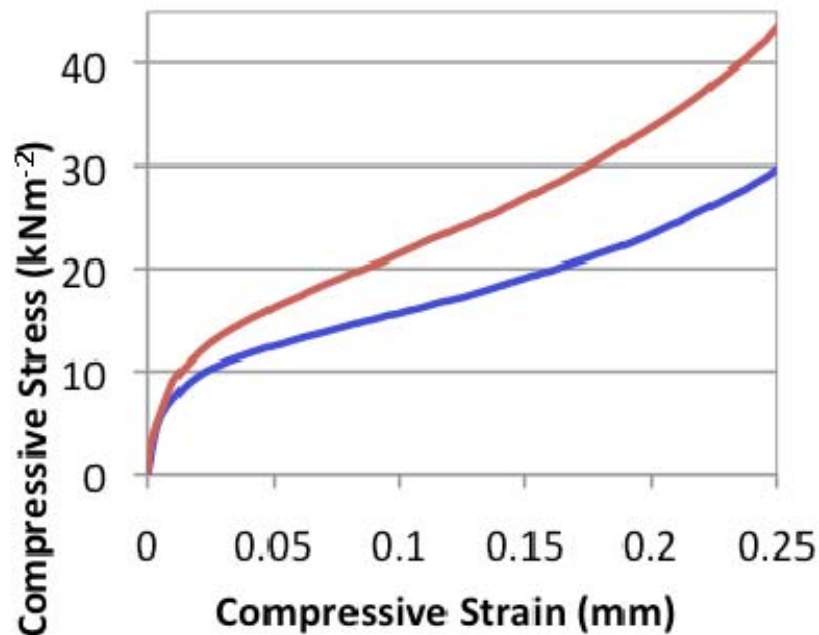
(a)
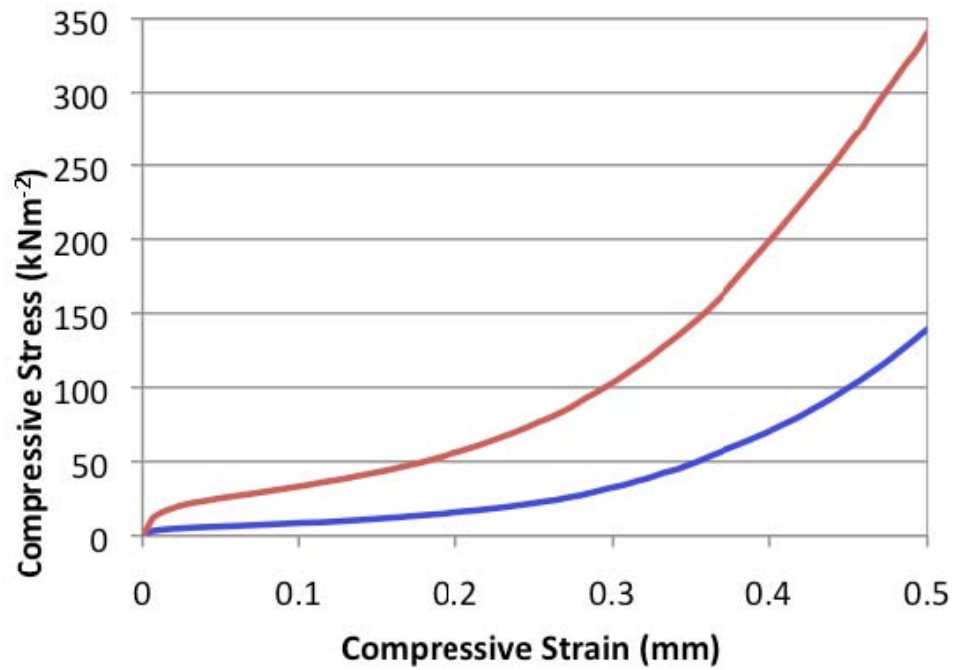
(b)
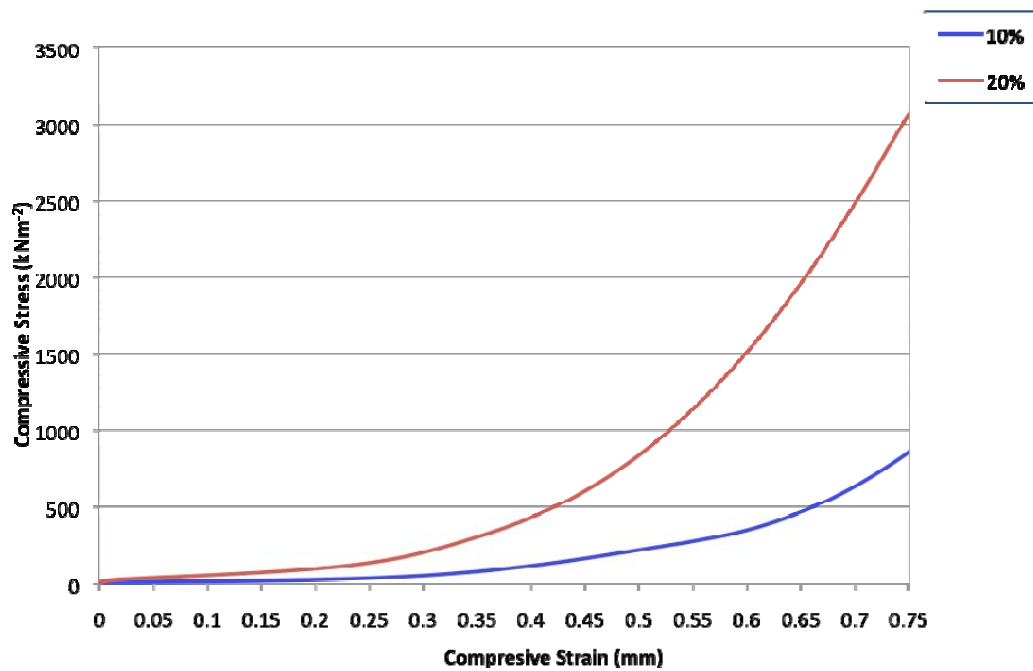
(c)

Figure 4.5. Compressive Stress versus Strain for (a) 25% compression,
(b) 50% compression and (c) 75% compression.

In general, the maximum compressive stresses plotted by the MR fluids under compression of 75% were significantly higher as compared to two other compression tests. For 10% volume fraction of CIP, the compressive stresses recorded at 30 kNm^{-2}, 140 kNm^{-2} and 850 kNm^{-2} for compression of 25%, 50% and 75%, respectively. Similarly, for 20% volume fraction of CIP, the compressive stresses were at 43 kNm^{-2}, 340 kNm^{-2} and 3100 kNm^{-2}. In comparison, the compressive stress recorded under the compression of 75% for both 10% and 20% volume fraction of CIP was 6 and 9 times, respectively, were higher than the value under compression of 50%. Impressively, the ration between the compressive stress recorded under the compression of 75% and 25%, was 28 and 72, for respective 10% and 20% volume fraction of CIP.

The particle distributions in the MR fluids under the compression tests were explained in the next results. In order to figure out the percentage of CIP in the specimens, the total area of particles inside the SEM image was divided into areas of the image, using equation 4.1. The total area of iron particles and area of images were computed easily by using the Image-J software and an example of computed SEM image illustrated in figure 4.6.

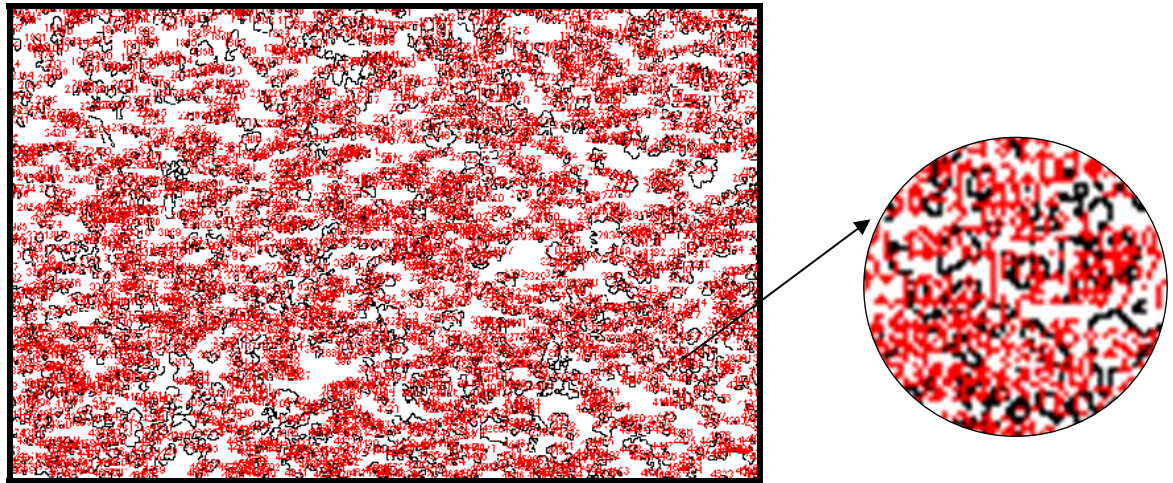Particle of particles = (Σ Particle area / Area of image) %   (4.1)

Figure 4.6. Particles distribution of 20% volume fraction of CIP under compression of 25% was computed by Image-J.

The percentage of particle distribution inside the SEM images for 'on' state and under compression of 25%, 50% and 75% is shown in table 4.2. For 10% volume fraction of CIP in the MR fluids, the percentage of particles distribution on the cross-section specimen showed a gradual increased, from 9.9% in 'on' state, followed by 11.1%, 15.3% and 23.6% under compression of 25%, 50% and 75%, respectively. On the other hand, the percentages of particle distribution on the top (centre) and top (side) have showed slight increased under the compression of 50% and 75%. In 'on' state and under compression of 25%, the percentages were not much different.

The increment percentage of the particle distribution for 20% volume fraction of CIP in the MR fluids was more significant. Without compression, the percentage of particle distribution on the cross-section of the specimens was 24.1%, and the percentage increased slightly when the fluid compressed to 25%. However, under compression of 50% and 75%, the percentage recorded impressive increased to 31.1% and 45.1%, respectively. The trend was also similar for the percentage of particle distribution on the top (centre) and top (surface) of the specimens. However, under compression of 50% and 75%, the percentage computed on the top (side) were significantly greater than on the top (centre).

Table 4.2. Percentage of particle distribution at 'on' state and under compression of 25%, 50% and 75%.

Volume Fraction of CIP	Percentage of particle distribution (%)											
	'On' state			Compression of 25%			Compression of 50%			Compression of 75%		
	Specimens			Specimens			Specimens			Specimens		
	T-C	T-S	C-S	T-C	T-S	C-S	T-C	T-S	C-S	T-C	T-S	C-S
10 %	17.9	17.5	9.9	17.1	19.0	11.1	19.7	20.5	15.3	21.7	23.9	23.6
20 %	22.0	21.1	24.1	21.2	22.2	25.0	24.7	35.7	31.1	27.1	43.1	45.1

Note : T-C : Top (centre), T-S : Top (side) and C-S : Cross Section.

Another important SEM images analysis was the column diameter formed by iron particles. The column formed when a magnetic field was applied to an MR fluid, which was consisting of numerous of single chain structures of iron particles. By utilising Image-J software, the average of the columns diameter could be computed by measuring the diameter of existing columns in the specimens. Thereby the average of the column diameter could be simply calculated.

The averages of column diameter in the MR fluid in 'on' state and under compression of 25%, 50% and 75% are shown in table 4.3. Generally, the averages of column diameter computed on the top (centre) and top (side) of the specimens for both volume fraction of CIP, showed a gradual increased in line with the level of compression. For example, for 20% volume fraction of CIP, the average of column diameter computed on the top (centre) was 40.2 µm at 'on' state condition. The averages of column diameter were enlarged to 43.2 µm, 47.9 µm and 52.6 µm under compression of 25%, 50% and 75%, respectively. The values recorded for top (centre) and top (side) showed only a slight different in term of column sizes.

Table 4.3. Averages of column diameter in 'on' state and under compression of 25%, 50% and 75%.

Volume Fraction of CIP	Average of column diameter (µm)											
	'On' state			Compression of 25%			Compression of 50%			Compression of 75%		
	Specimens			Specimens			Specimens			Specimens		
	T-C	T-S	C-S	T-C	T-S	C-S	T-C	T-S	C-S	T-C	T-S	C-S
10 %	23.3	22.5	19.6	26.0	27.4	23.3	30.7	29.1	-	37.9	35.3	-
20 %	40.2	39.6	29.2	43.2	39.0	32.1	47.9	45.1	-	52.6	48.7	-

Note : T-C : Top (centre), T-S : Top (side) and C-S : Cross Section.

Meanwhile, the average column diameter of the cross-section specimens could be computed for 'on' state and compression of 25%, where also showed an enlargement. Unfortunately, the columns of the SEM images of cross-section specimens for compression of 50% and 75% could not be identified due to the particles distributions were very compact. Therefore no average of column diameter was computed. For an example, the SEM image of cross-section specimen for 20% volume fraction of CIP under compression of 75% is shown in figure 4.7.
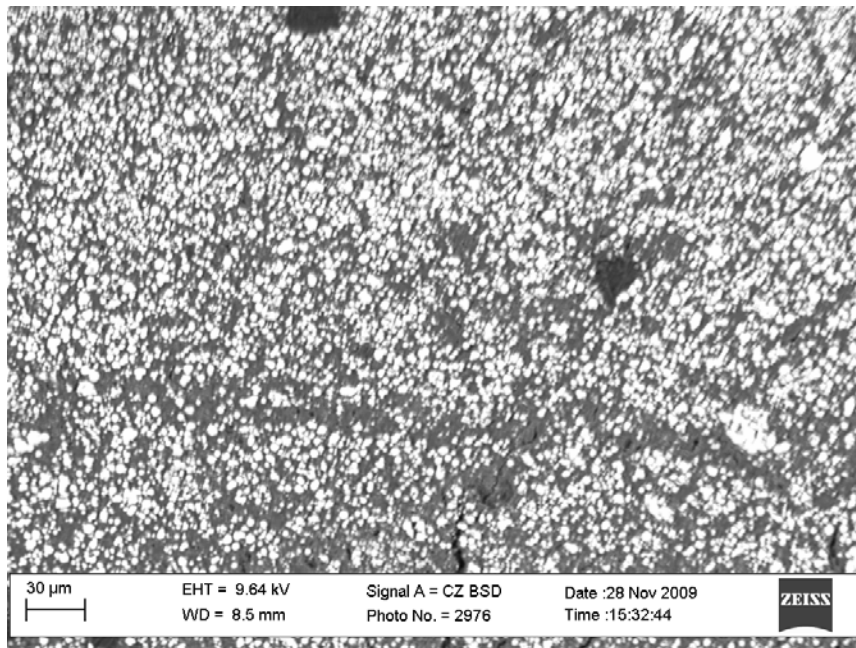

Figure 4.7. SEM image of cross-section specimen for 20% volume fraction of CIP under compression of 75%.

The discussion of the compression tests and analysis of SEM images will be commenced with a brief explanation about the behaviour of MR fluids in 'on' state. Subsequently, the behaviour of the MR fluids under compression will be discussed further in term of microscopic aspects particularly on the particle distribution and column formation.

Without an induction of magnetic field, the iron particles in an MR suspension were distributed randomly in the carrier fluid. However, with the presence of an external magnetic field, the iron particles polarized and formed chain-like structures. Ideally, the particle chains distributed perpendicularly over the space between two plates, and the end chains adhere to the plates. The formation of the chain-like structures occurred drastically and each particle in the suspension took a fixed position in the closed chains. It can be assumed that the length of the chain was equal to the gap between the two plates. Furthermore, it also could be deduced that without compression, the column formation still not occurred and the particles only formed single chains.

In the compression tests, the test rig was designed for the squeeze mode application. The physical model of the MR fluids under compression is illustrated in figure 4.8.
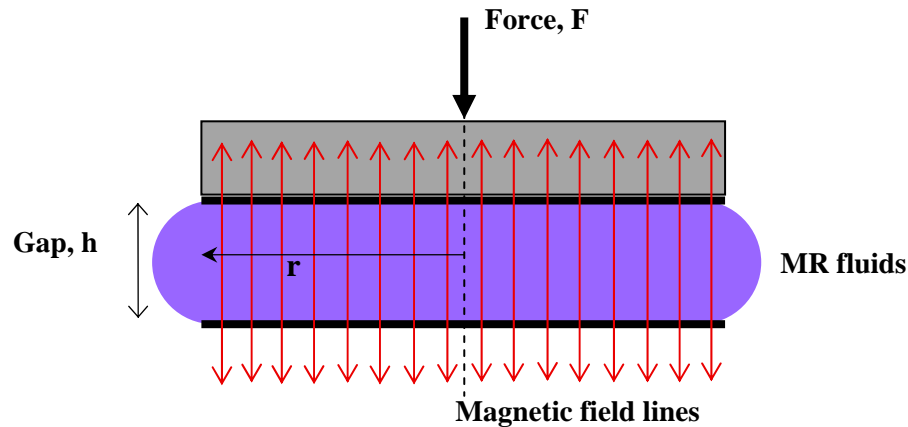

Figure 4.8. The physical model of the MR fluid under compression.

Therefore, the compressive stress, P in the compression tests can be represented as

$$P = F/A = F/\pi r^2 \tag{4.1}$$

where F is the compressive force, A is the surface area of compression and r is the radius of the cylinder. Meanwhile, the compressive strain is simply represented by the value of the strain. However, in the compression tests, the solely form of stress experienced by the epoxy-based

MR fluid was volumetric stress. Accordingly, the MR fluid experienced volumetric strain, which was associated to the compressibility of the material. Therefore, the relation between volumetric stress and strain could describe the volumetric change or tendency of the fluid to deform under pressure. As an analogy to the solid, the volumetric stress would be better to be referred as an apparent compressive stress.

Since the volumetric stress was a pressure based, the MR fluid experienced dissimilar levels of pressure in the gap, which rely on its position. The pressure took place at the centre of the cylinder was more intense and greater as compared to the pressure acted nearly the outside cylinder, which was closed to atmospheric pressure. As a result, the fluid moved towards outside of the cylinder and the only resistant was the viscosity of the fluid. This explanation brought to a conclusion that the compressive strain or change of the displacement affected mostly to the behaviour of the MR fluids.

Prior to the compression tests, the MR fluid behaved like a semi-solid material due to the formation of chain-like structures in between the cylinders. At this point, the values of compression stress recorded were very small and almost zero, by reason of no internal reaction from the fluids. When the upper cylinder started to lower down from the initial gap to the lower cylinder with a constant speed, the liquid particularly the chain-like structures of the iron particles reacted as a barrier to the compression. The internal reaction of the fluid represented the degree of compressive stress to the MR fluid. The level of the internal reaction increased in conjunction with the increased of compressive strain, and as a result, the recorded compression stress has showed a gradual increased. At the same time, volume of the MR fluids between the gaps has decreased. Therefore the composition of the MR fluid was dissimilar to its original volume. Since the iron particles hold in the chain structures, it was assumed that the carrier fluid, i.e. the epoxy was being expelled. The movement of the epoxy towards outside of the cylinder was relatively slow due to the obstacles created by the chains. Based on this assumption, it could simply be computed that the composition of the MR fluid has decreased in the samples of epoxy-based MR fluids. Simultaneously, the volume fractions of CIP in the specimens also changed and the new calculated percentages for both 10% and 20% of initial volume fraction of CIP are shown in table 4.4 and 4.5.

Table 4.4. The new volume fractions of 10% initial volume fraction of CIP in the specimens for compression of 25%, 50% and 75%.

Parameters	Total Volume	Composition			Volume Fraction of CIP
		CIP	Resin	Hardener	
Initial Volume	2 ml	0.2 ml	1.5 ml	0.3 ml	10 %
			= 1.8 ml		
Compression of 25%	1.5 ml	0.2 ml	1.3 ml		13.3 %
Compression of 50%	1.0 ml	0.2 ml	0.8 ml		20 %
Compression of 75%	0.5 ml	0.2 ml	0.3 ml		40 %

Table 4.5. The new volume fractions of 20% initial volume fraction of CIP in the specimens for compression of 25%, 50% and 75%.

Parameters	Total Volume	Composition			Volume Fraction of CIP
		CIP	Resin	Hardener	
Initial Volume	2 ml	0.4 ml	1.334 ml	0.266 ml	20 %
			= 1.6 ml		
Compression of 25%	1.5 ml	0.4 ml	1.1 ml		26.7 %
Compression of 50%	1.0 ml	0.4 ml	0.6 ml		40 %
Compression of 75%	0.5 ml	0.4 ml	0.1 ml		80 %

As can be seen from tables 4.4 and 4.5, the volume fraction of CIP in the specimens was expected to be double under compression of 50% and to be quadruple under compression of 75%. However, under compression of 25%, it could be assumed that only a small volume of epoxy was being expelled from the testing area, thus the increased of volume fraction of CIP were slightly small. The changes in the composition and volume fraction were also in line with the increased in the percentage of particle distribution of MR fluids as shown previously in table 4.2, although the numbers were not rather accurate. Thus, the small percentage of volume fraction of CIP indicated that a small volume of CIP also being expelled along with the carrier fluid at the beginning of compression (25%).

The decreased in the volume of MR fluid could refer to the increased in volume fraction of CIP or the increased of particle distribution in the MR fluids, which gave some explanation to the exponential increases plotted by the compressive stresses after the compression of 25% has been reached. There was an assumption made by some researchers stated that the degree of magnetization of the magnetic particles in the MR fluids in response to a magnetic field was relative to their volume fraction [31]. Further assumption could be made that the higher the volume fraction in the MR fluids, the higher the tendency of the iron particles to move and fixed themselves along the lines of magnetic flux. As a result, greater resistant were formed and higher compressive stress would be produced. Furthermore, in this experiment, the samples of 'on' state were executed by cyclic tests before the solidification process took place. Thus, the columns in the specimens of 'on' state could be clearly observed. When the MR fluids compressed with a constant speed, the columns became shorter and were pushed closer to form compact structures. For that reason, the SEM analysis showed that the averages of column diameter for specimens of MR fluids under compression of 75% were significantly larger. On the other hand, for all specimens, the averages of column diameter computed on cross-section were always smaller than on the top specimens. This explains that the columns were not uniform in size, where the sizes of the columns at both ends were much ticker than in the middle, which may also contribute to the strength of the fluid. Tao et al. [20-21] discovered from their SEM analysis of epoxy based MR fluids, that under compression, the ends column sizes were much thicker as compared to the size in the

middle. They explained that the phenomenon occurred as a result of the attraction between the chains became stronger and pulled these chains rapidly together, after the MR fluid was compressed. Therefore, such structures were robust as a result of the microstructure of MR fluids was greatly changed. The column formation between the gaps is illustrated in figure 4.9.

(a)   (b)

Figure 4.9. Formation of columns (a) before compression and (b) after compression.

Consequently, those factors in which influenced the compression behaviour of the MR fluids are illustrated in figure 4.10. This figure demonstrated that the increased of the compressive stresses were resulting the increased of the volume fraction of CIP. Accordingly, the particles distribution and column size of the MR fluids have increased throughout the compression as well.
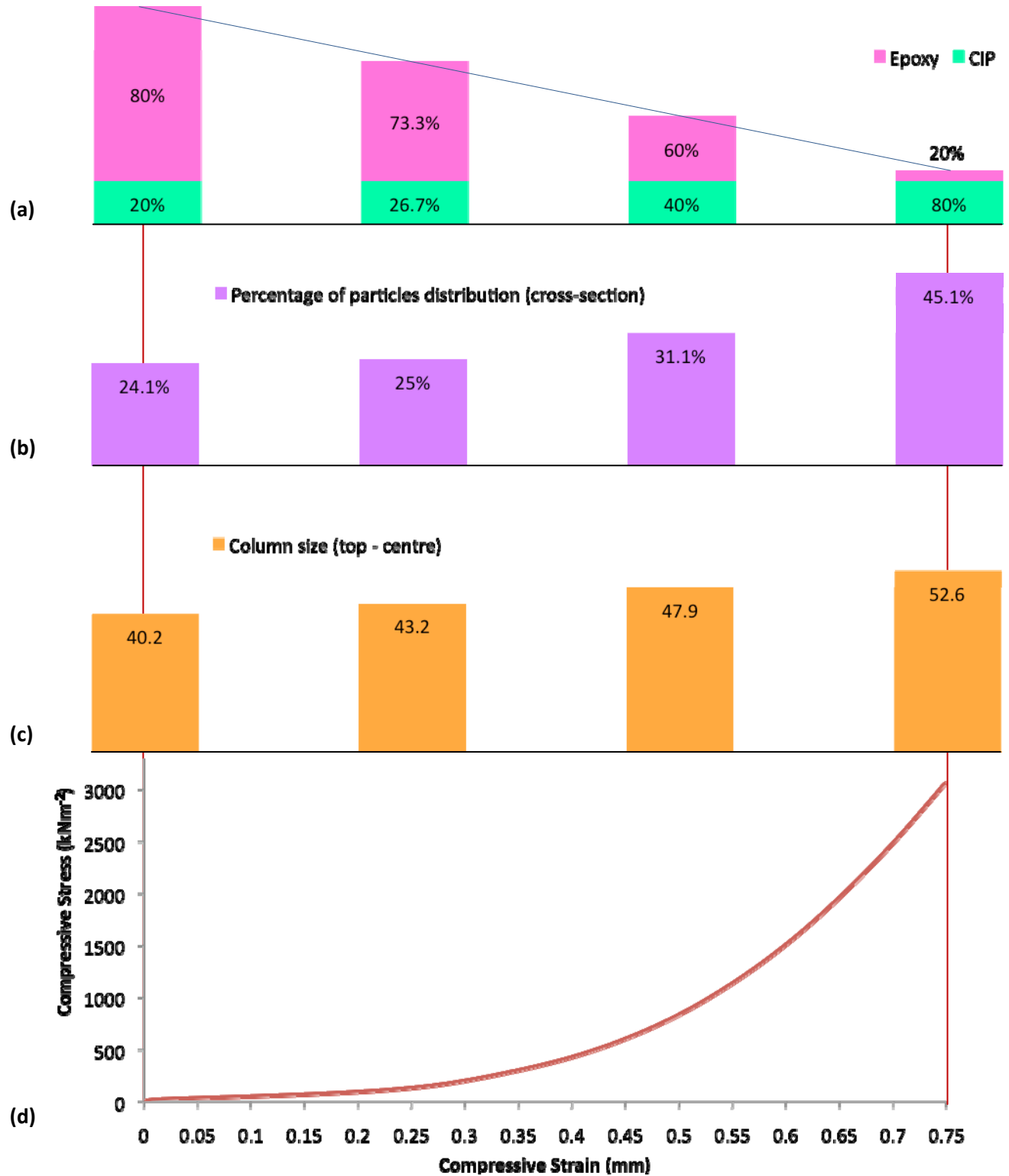
Figure 4.10. Compression behaviour of MR fluids (a) volume fraction of CIP, (b) percentage of particles distribution (cross-section), (c) average of column size (top centre), and (d) compressive stress versus strain.

CHAPTER 5

CONCLUSION

Magnetorheological (MR) fluids operated in squeeze mode have unique features as a result of its ability to produce much higher compressive and tensile stresses. This research has identified the compression behaviour of MR fluids under squeeze mode. The first study in this project was the rheological behaviour of an epoxy-based MR fluid. Subsequently, compression tests for 25%, 50% and 75% have been conducted in order to investigate the stress-strain relationships of MR fluids under compression in squeeze mode. Finally, the microstructures of the MR fluids specimens for 'off' state, 'on' state and under compression were examined by Scanning Electron Microscopy (SEM) and analysed by using Image-J software. Several conclusions from this project can be highlighted as follows:

(1)   The rheological behaviour of an epoxy-based MR fluid was observed by conducting viscosity tests. As a benchmark, the viscosity of a neat epoxy (resin and hardener) has been examined first. The viscosity of the neat epoxy has shown an exponential increase over time. In contrast, the viscosities of an epoxy-based MR fluid have decreased in the first 30 minutes (for 10% volume fraction of CIP) and 40 minutes (for 20% volume fraction of CIP), before showing an exponential increase until they were cured completely. By introducing the carbonyl iron powder (CIP) into the epoxy, the change of the mixture density as well as the occurrence of chemical reaction influences the polymerization process in the compounds.

(2)   The compression behaviour of the epoxy-based MR fluid in term of stress-strain relationships was examined throughout compression tests of 25%, 50% and 75%. Both of the 10% and 20% volume fraction of CIP have shown a similar trend, which was a drastic increased for the first 0.01 mm strain, followed by a gradual increased until 0.25 mm and eventually an exponential curve until 0.75 mm strain was reached. For that reason, the compressive stresses recorded under compression of 75% were significantly higher than under compression of 50%. Meanwhile, under compression of 25%, the compressive stress showed only a slight increased in comparison. The compressive stresses plotted by 20% volume fraction of CIP were always higher than 10% volume fraction of CIP. Therefore, the higher the volume fraction of CIP and the compressive strain, the higher compressive stress of MR fluids would be achieved.

(3)   The specimens produced in the compression tests were examined by SEM and analysed by using Image-J software. During compression, the volume fractions of the MR fluids have shown an increased as a result of relative decreased in the sample composition. For this reason, in the microstructure analysis, the particles distributions and column sizes of the specimens were found to increase in conjunction with the compression and recorded a significant value under compression of 75%. This microstructure study proves that during the compression, most of the iron particles were hold in the fluids while the epoxy was expelled out of the cylinder. In addition, the epoxy-based MR

fluid in this study was reliable and could be used in further research of MR fluids microstructure.

This study might serve as a platform for future studies in the compression behaviour of MR fluids in squeeze mode. Therefore, some recommendations for future work are outlined as follows:

(a)   Further investigation of the phenomenon regarding the relative movement between the solid particles and the carrier liquid in the MR fluid during the compression and tension processes. This could be done using scanning electron microscopy (SEM) to estimate the average particle size, particle size distribution, shape and surface morphology of the particles.

(b)   It would be interesting to model the field-responsive behaviour of MR fluids to describe the mechanism of stress formation during the compression and tension processes. The model would assist characterizing the physics behind the interaction between the solid magnetic particles and the magnetic field and may help developing new materials with improved performance.

(c)   Further improvement of the test rig design where the volume of tested materials would be constrained in the gap between the two flat parallel surfaces. The new design could be achieved by avoiding the clearance, in this case, the gap between the outer diameter of the upper cylinder and the inner diameter of the support cylinder. Therefore, this arrangement could be adopted to deal effectively with the compression and tension processes.

(d)   To investigate the achievable stresses when two working modes, such as compression and shear modes combined. The process is called compression-assisted-aggregation and it employs forcing MR fluid to form a new microstructure that is much stronger than the existing structure.

CHAPTER 6

RESEARCH OUTPUT

6.1   Citation Details of Articles

1.   I. Ismail, **S.A. Mazlan** and A.G. Olabi, Magnetic Circuit Simulation for Magnetorheological (MR) Fluids Testing Rig in Squeeze Mode, Advanced Materials Research, Vols. 123-125, 2010, 991-994.

2.   I. Ismail, **S.A. Mazlan** and A.G. Olabi, Experimental Study on Fluid-Particle Separation of Magnetorheological (MR) Fluid in Squeeze Mode, *Submitted to Journal "Smart Materials and Structures".*

3.   **S.A. Mazlan,** I. Ismail and A.G. Olabi, Compressive and Tensile Stresses of Magnetorheological Fluids in Squeeze Mode, *"Submitted to International Journal for Applied Electromagnetics and Mechanics".*

6.2   Citation Details of Conference Papers

1.   I. Ismail, **S.A. Mazlan** and A.G. Olabi, Experimental Study on the 'Squeezing Effect' of Magnetorheological (MR) Fluid, in proceedings of the Workshop and International Conference on Smart Materials, Smart Materials: Theory and Applications, Dublin, Ireland, ISBN 1872327907, September 22-24, 2010, 31-35.

2.   **S.A. Mazlan**, I. Ismail and A.G. Olabi, Smart Materials: Field-Responsive Fluids, in proceedings of the Workshop and International Conference on Smart Materials, Smart Materials: Theory and Applications, Dublin, Ireland, ISBN 1872327907, September 22-24, 2010, 48-51.

6.3   Citation Details of Presentation

1.   I. Ismail, **S.A. Mazlan** and A.G. Olabi, Investigation of Fluid-Particle Separation Phenomenon of Magnetorheological Fluid under Compression Mode, Presented in the UK-Malaysia-Ireland Engineering Science Conference, Belfast, Northern Ireland, UK, June 23-25, 2010.

CHAPTER 7

HUMAN CAPITAL DEVELOPMENT

None

CHAPTER 8

AWARDS / ACHIEVEMENT

None

REFERENCES

[1]   Olabi, A. G. and Grunwald, A., (2007), "Design and Application of Magneto-Rheological Fluid", *Materials and Design*, Vol. 28 (10), pp. 2658-2664.

[2]   Norbert, G., (2007), *Magneto-Rheological Fluids in Squeeze Mode*, Verlag Dr. Muller, Saarbrücken, Germany.

[3]   Mazlan, S. A., (2008), "The Behaviour of Magnetorheological Fluids in Squeeze Mode", Ph.D. Thesis, Dublin City University, Ireland.

[4]   Ahmadian, M. et. al., (2009), "Magneto-rheological fluid behavior in squeeze mode", *Smart Materials and Structures*, Vol. 18 (9), 095001

[5]   Tian, Y., et al., (2002), "Electrorheological Fluid Under Elongation, Compression, and Shearing" *Physical Review E*, Vol. 65 (3), 031507

[6]   Pradeep, P. P., (2001), "Magnetorheological fluids : Principle and applications", *Smart Materials Bulletin*, pp. 7-10

[7]   Seval, G., (2002), "Synthesis And Properties Of Magnetorheological (Mr) Fluids", Ph.D. Thesis, University of Pittsburgh, USA.

[8]   Scherer, C. and Neto, A. M. F., (2005), "Ferrofluids: Properties and Applications", *Brazilian Journal of Physics*, Vol. 35 (3A), pp 718-727

[9]   Ferrotec (USA) Corporation, [online], www.ferrotec.com, [Accessed 21 November 2009]

[10]   Bansbach Easylift International (Germany), [online], www.bansbach.com, [Accessed 21 November 2009]

[11]   Kciuk, M. and Turczyn, R., (2006), " Properties and application of magnetorheological fluids", *Journal of Achievements in Materials and Manufacturing Engineering*, Vol. 18 (1-2) pp. 127-130

[12]   Lord Corporation (USA), [online], www.lord.com, [Accessed 25 November 2009]

[13]   Wang, J. and Meng, G., (2002), "Magnetorheological fluid devices: principles, characteristics and applications in mechanical engineering", *Journal of Materials : Design and Applications*, Vol. 215 (L) pp. 165-174

[14]   Rabinow, J. (1948), "The magnetic fluid clutch", *Transactions of the AIEE*, Vol. 67 (2), pp. 1308-1315

[15]   Bose H. and Trendler A., (2003), "Smart Fluids - Properties and Benefit for New Electromechanical Devices", *AMAS Workshop on Smart Materials and Structures*, *SMART'03, Jadwisin*, pp. 329-336

[16]   BASF, The Chemical Company, [online], www.basf.de, [Accessed 23 November 2009]

[17]   Douglas J. F., Gasiorek J. M. and Swaffield J. A., (1995), *Fluid Mechanics*, 3rd Ed., Longman Scientific & Technical, Harlow Essex, UK.

[18]   Goncalves, F. D., (2005), " Characterizing the Behavior of Magnetorheological Fluids", Ph.D. Thesis, Virginia Polytechnic Institute and State University, USA

[19]   Ahmadian, M. et al., (2009), "Non-dimensional Modeling and Experimental Evaluation of a MR Squeeze Mode Rheometer", *Journal of Physics*, Vol. 149 (1), 012048

[20]   Tao, R., (2001), "Super-strong magnetorheological fluids", *Journal of Physics*, Vol. 13, pp. 979-999

[21]   Tao, R. et al. (2000), "Structure-enhanced yield stress of magnetorheological fluids", *Journal of Applied Physics*, Vol. 87 (5), pp. 2634-2638
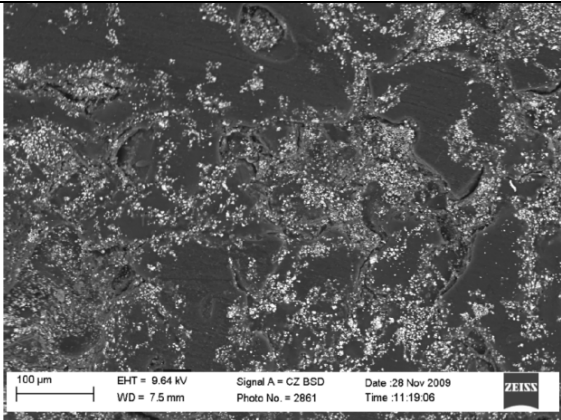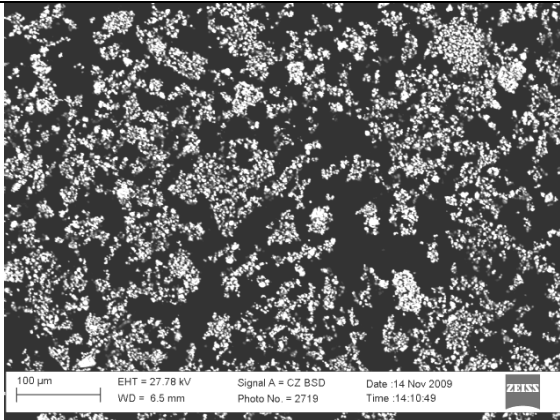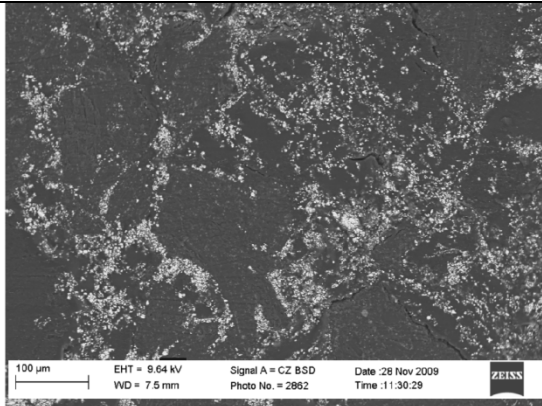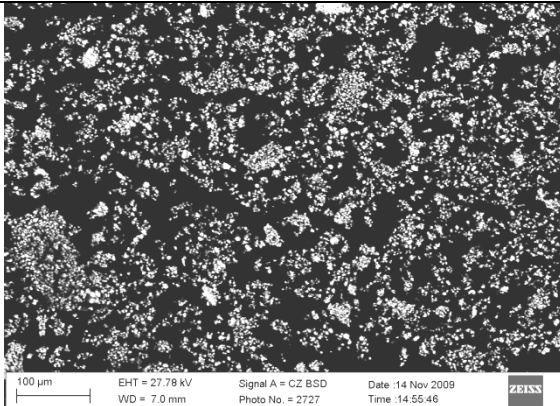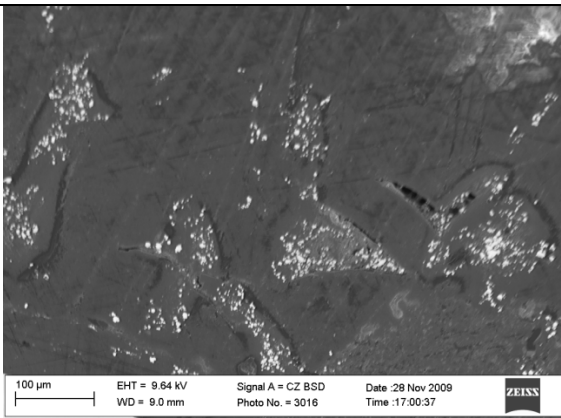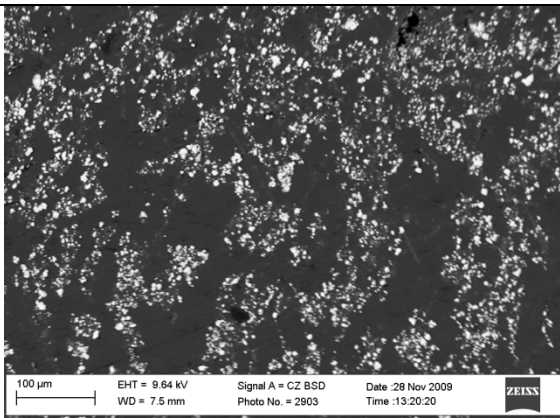
[22] Choi, H. J. et al, (2004), "Magnetorheological characterization of carbonyl iron based suspension stabilized by fumed silica", *Journal of Magnetism and Magnetic Materials*, Vol. 282, pp. 170-173

[23] Brandon, D. and Kaplan, W. D., (2008), *Microstructural Characteristerization of Materials*, (2nd Edition), Wiley, England

[24] Jansen, M.P.M., (2007), "Visualization of a MR-fluid", Eindhoven University of Technology, Netherland

[25] Carl Zeiss International, [online], www.zeiss.com [Accessed 27 November 2009]

[26] Ouellette, J. (2005), " Smart Fluids Move into the Marketplace", *The Industrial Physicist*, pp. 14-17

[27] Spencer, B. F., (2003), "State of the Art of Structural Control", *Journal of Structural Engineering*, pp. 645-865

[28] Zeiss Evo ® MA and LS series Scanning Electron Microscopes Operator User Guide

[29] Vieira, S. L. et al., (2003), "Behaviour of MR Fluids in Squeeze Mode", *International Journal of Vehicle Design*, Vol. 33 (1-3), pp. 36-49

[30] Rimlyand, V. I., Starikova, V. N. and Bakhantsov, A. V. (2009), "Investigation Into The Dynamics Of Physical Properties Of An Epoxy Resin During Solidification", *Russian Physics Journal*, Vol. 52 (5), pp. 532-540

[31] Jolly, M. R., Bender, J. W. and Carlson, J. D., (1999), "Properties and Applications of Commercial Magnetorheological Fluids", *Journal of Intelligent Material Systems and Structures*, Vol. 10 (1), pp. 5-13

.

APPENDICES
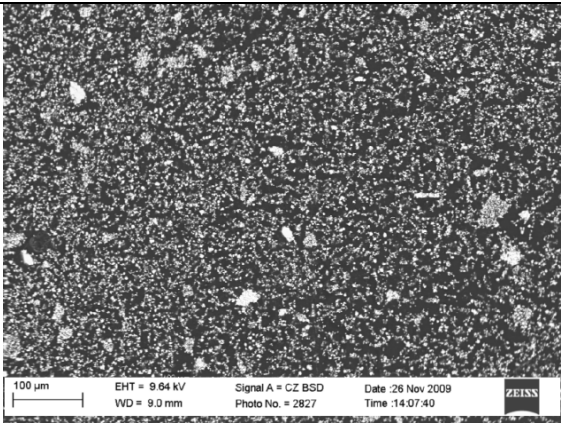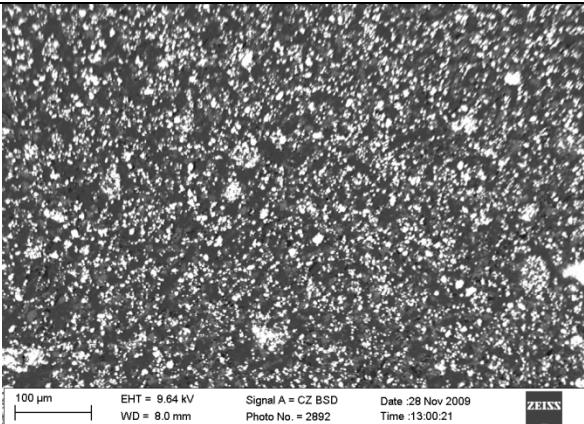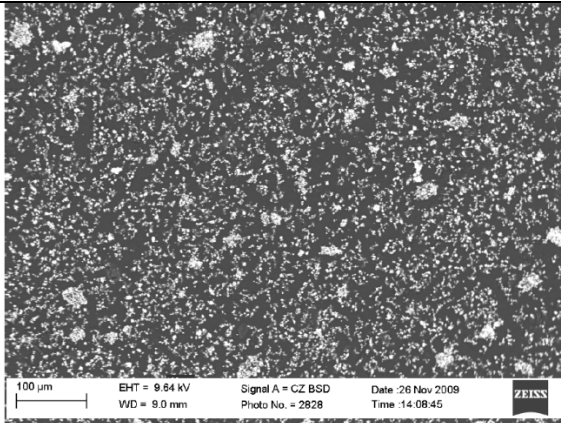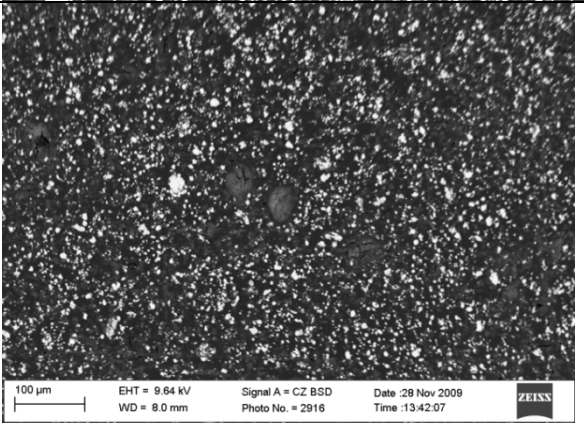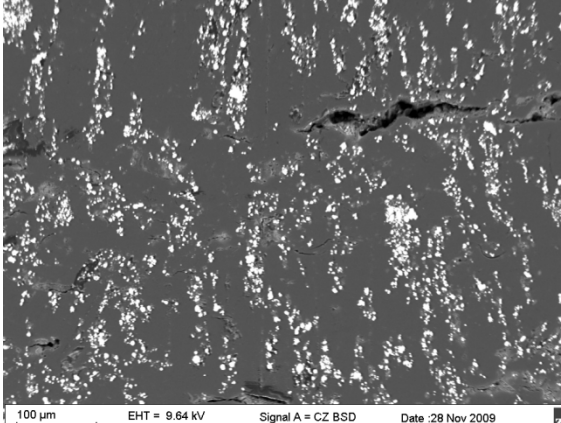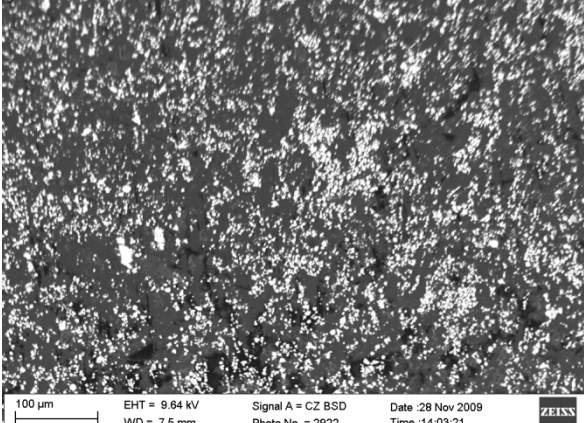
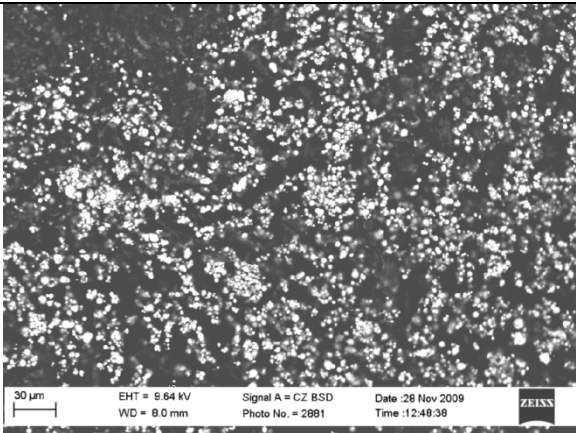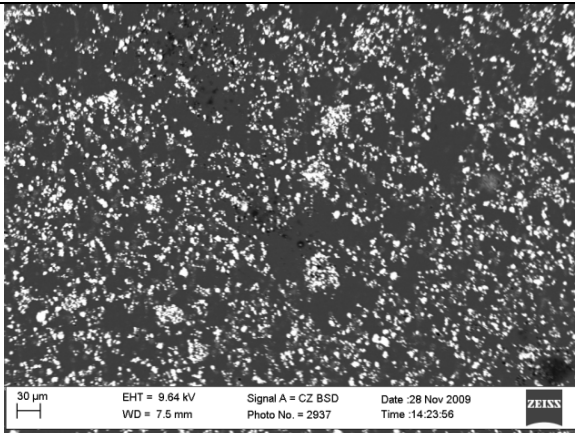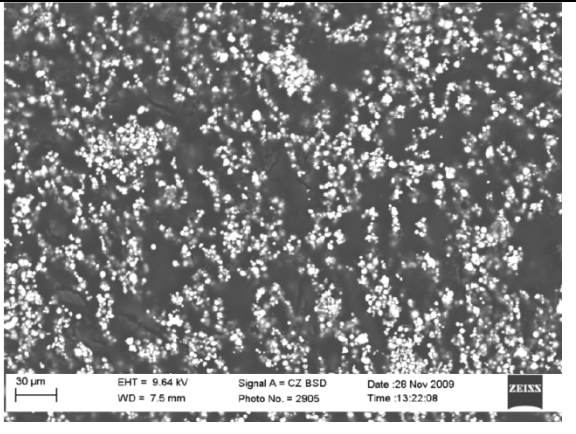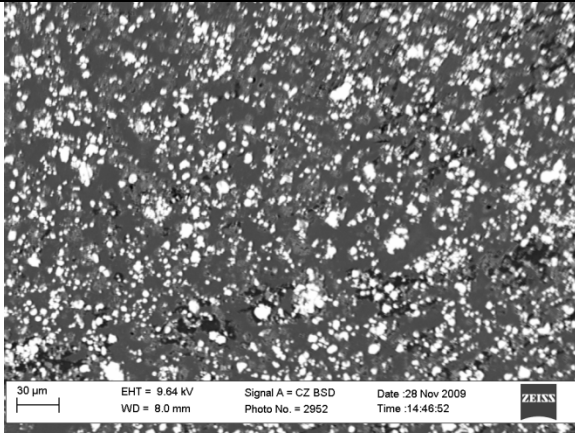Appendix A. The stress-strain relationships of MR fluids under compression.

Compression of 25%

Compression of 50%

Compression of 75%
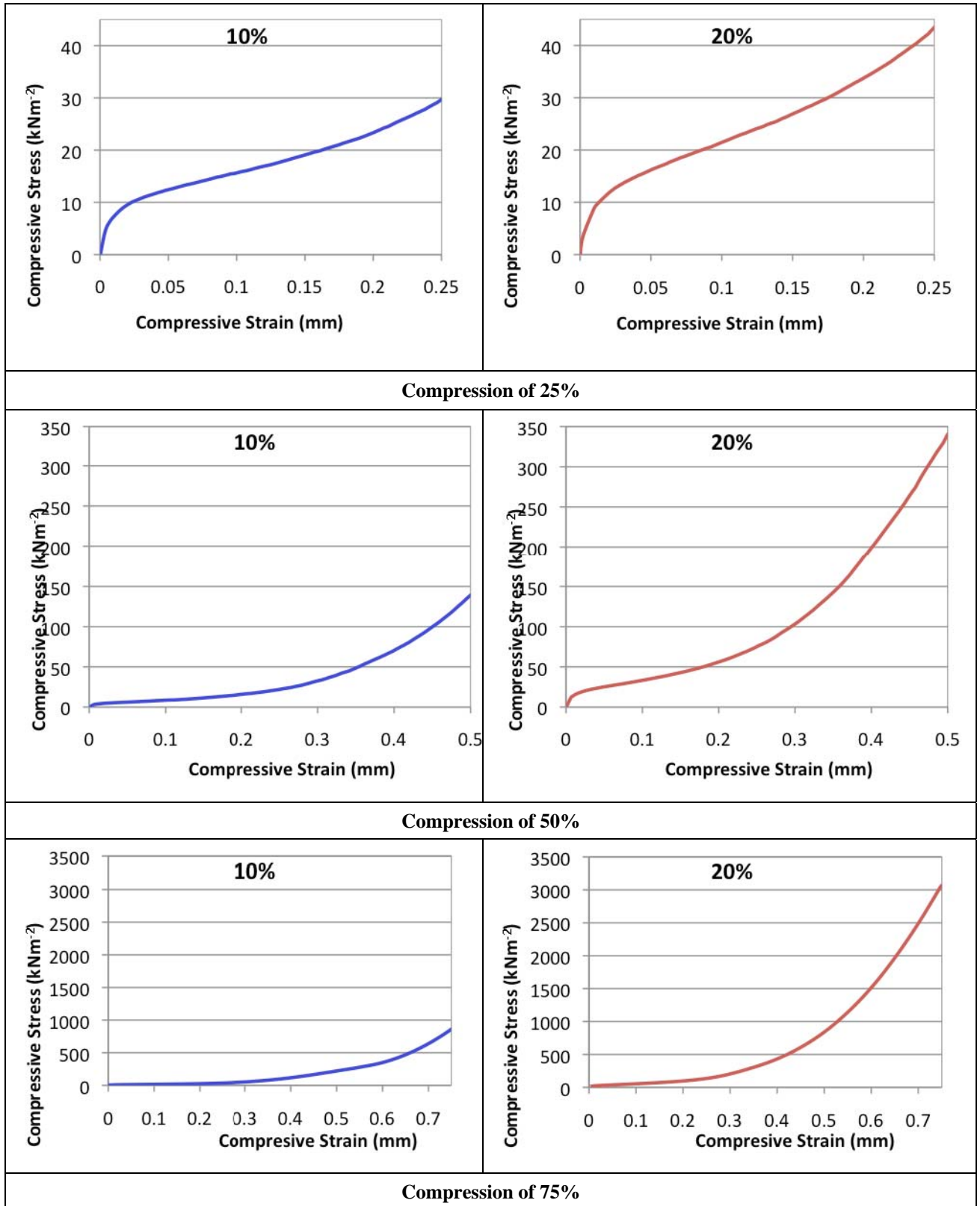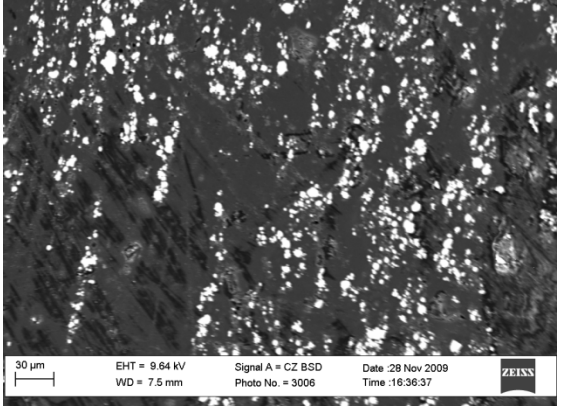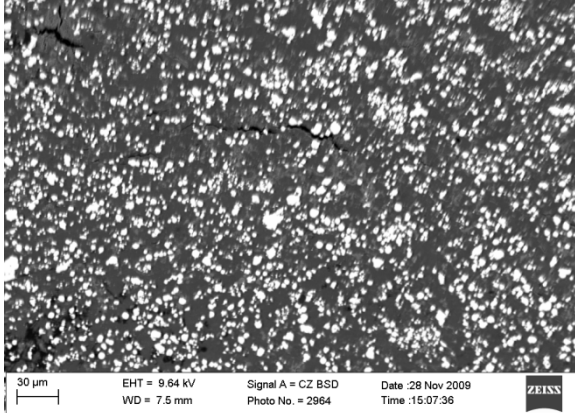
Appendix B1. The SEM images of epoxy based MR fluids in 'off' state.

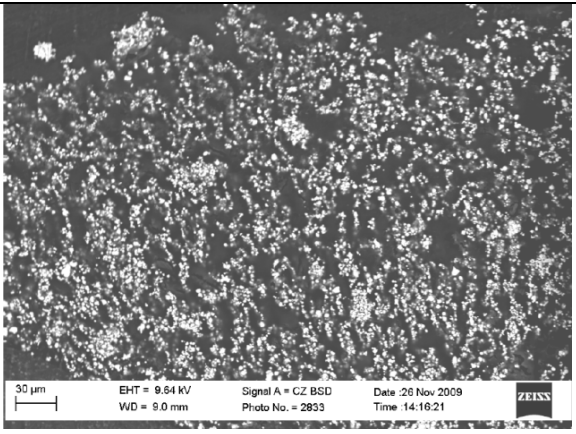|	10% CIP	20% CIP
A		
B		
C		
Notes: A – Top (centre), B – Top (side), C – Cross-section		
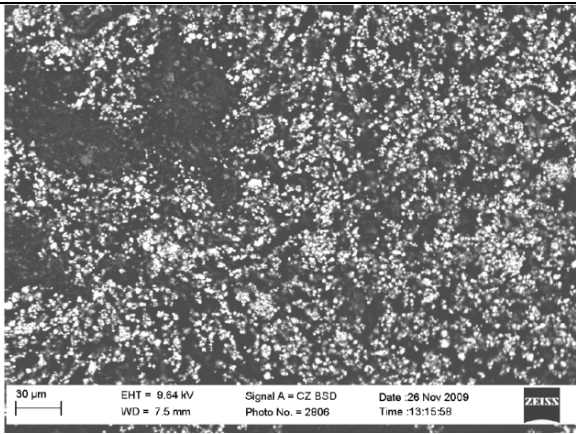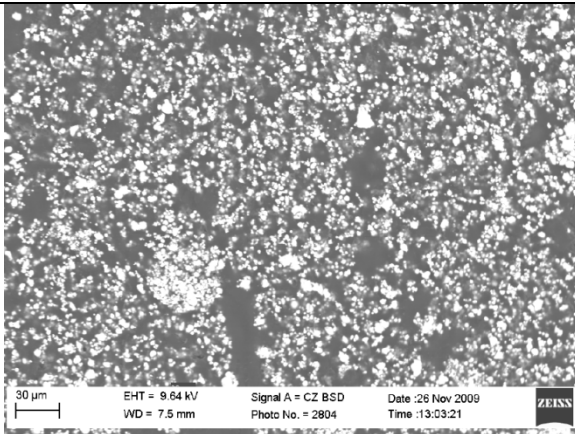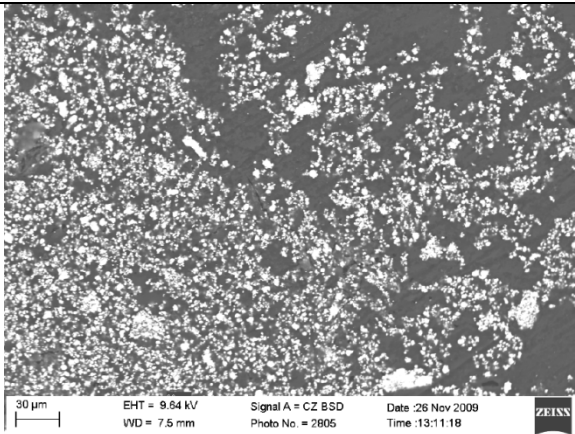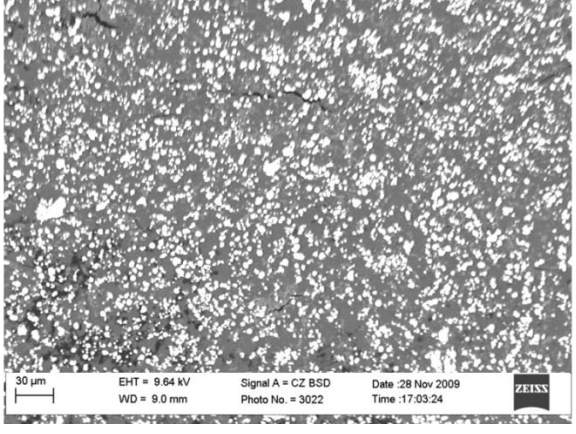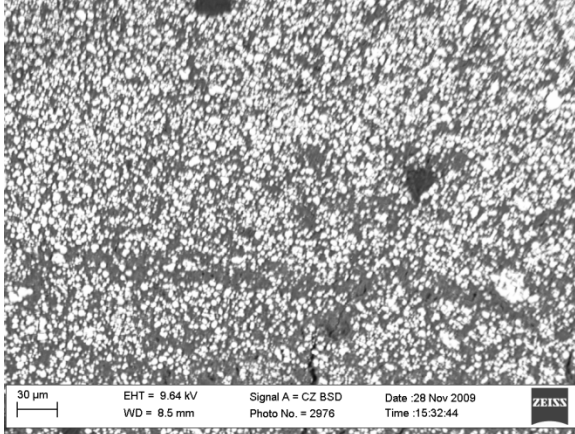
Appendix B2. The SEM images of epoxy based MR fluids in 'on' state.

	10% CIP	20% CIP
A		
B		
C		
Notes: A – Top (centre), B – Top (side), C – Cross-section		

Appendix B3. The SEM images of epoxy based MR fluids under compression of 25%.

	10% CIP	20% CIP
A		
B		
C		
Notes: A – Top (centre), B – Top (side), C – Cross-section		

Appendix B4. The SEM images of epoxy based MR fluids under compression of 75%.

	10% CIP	20% CIP
A		
B		
C		
Notes: A – Top (centre), B – Top (side), C – Cross-section		